UNIVERSITY OF PADUA

Masters of Bioengineering for Neuroscience

Error Potential detection during driving operations of a powered wheelchair

Thesis supervisor:

Prof. Luca Tonin

Thesis by Gabriele Costaglioli

2018762

2021/2022

Contents

1. Introduction

Modern technologies allow people with motor impairment (e.g., paraplegia and tetraplegia) to improve their general wealth. Among the modern technologies there is one of particular interest, called brain-computer interface (BCI) that directly connect the brain with a machine for the execution of a specific task. This technology can be used to promote the implementation of a brain-controlled wheelchair, which would significantly increase the independence of people suffering from severe motor disabilities. From the literature regarding the employing of the BCI for the assistance of people emerges a lack of studies of an algorithm that can adjust the wheelchair's trajectory if a problem emerges. In order to improve this aspect, we analysed if a specific brain response generated when an unexpected situation occurs (error-related potential (ErrP)) is reliably detectable; the final goal of this research was to create an offline-algorithm for the classification of the brain responses in order to set a baseline for the implementation of a online-algorithm of trajectory correction.

The first chapter will present an overview of the BCI and the error-related potential and the possible applications of this technology. In the following chapters it will be highlighted the motivation and main point of focus of our research, along with the experimental protocol, the results obtained and the discussion of the results.

1.1 State of art

1.1.1 Brain-Computer Interface

The Brain-Computer Interface (BCI), also known as Brain-Machine Interface (BMI) is a system that decodes human brain signals to operate computers and various communication devices (Ramadan & Vasilakos, 2017). The following definitions are provided in the literature:

1) Donoghue et al. defined the BCI as a Brain Machine Interface (BMI), whose main purpose is to transmit commands from the cortex to physical objects like computers or robotic limbs that can control impaired body parts (Donoghue, 2002).

2) The BCI was described by Wolpaw et al. as a device that offers the brain a new, non-muscular communication and control channel (Wolpaw, 2002).

3) According to the definition given by Schwartz et al., the BCI is "Microelectrodes installed chronically in the cerebral cortex show promise for harnessing brain activity to control devices with enough speed and agility to substitute natural, lifelike motions in paraplegic individuals" (Schwartz, 2004).

According to these definitions, the BCI's overall functionalities include recording brain signals, analysing them, classifying them, and using them to control devices (Figure 1.1). In order to describe the communication between the brain and a computer or other external equipment, the terms BMI and BCI may be used interchangeably, in this thesis this system will be called BCI. People who have neuromuscular injuries and neurodegenerative disorders are directly impacted by the BCI. Amyotrophic lateral sclerosis, for example, disrupts nerve cells in the brain and spinal cord without impairing a person's cognitive ability (Ramadan & Vasilakos, 2017).

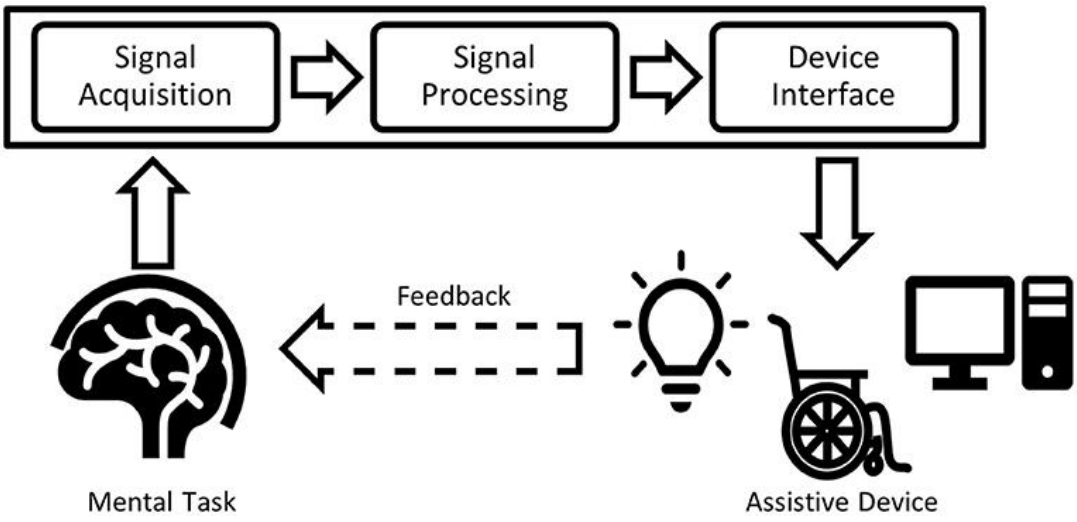

Figure 1.1 BCI loop

1.1.2 BCI classifications

BCI can be divided into categories based on intrusiveness, and synchronization. The BCI can be classified as invasive, non-invasive or semi-invasive and synchronous or asynchronous.

In an invasive BCI, microelectrodes are surgically inserted in the brain beneath the skull (Nakasaki et al., 1989). In this situation, the signal may have been recorded with good quality, but it may have been susceptible to scar tissue build-up over time, leading to signal loss. Additionally, it is impossible to relocate the intrusive technology to measure different areas of the brain once they have been implanted (D. Tan & Nijholt, 2010). In contrast, no scalp penetration occurs during non-invasive BCI when recording signals; usually electroencephalography (EEG) is used to capture the brain waves in the non-invasive BCI (Millan et al., 2004); non-invasive BCI is still overall preferred because it prevents surgery even though the signals might be of poor quality,

In the semi-invasive BCI the electrodes are placed beneath the skull, and electrocorticography (ECoG) is used to capture the brain waves. For instance, the Pfurtscheller group implanted macroelectrodes over the frontal areas of epileptic patients. The BCI system was able to categorize the visual tasks' ECoG within a single session as the patient sought to perform tasks involving the hands, mouth, and tongue (Birbaumer, 2006).

When a user interacts with a BCI system at a specific moment, the system is referred to as synchronous. In other words, the subject is forced to interact with the system

at a set time otherwise the system won't be able to analyse properly the intention of the subject. In contrast, the person can execute their mental tasks at any moment while using asynchronous BCI (Bashashati et al., 2007) (Scherer et al., 2007), and the system will respond to their mental actions. The subject is thus free to interact with the BCI at any moment.

1.1.3 Mental control signals classifications

BCI relies on brain-derived control signals for its operation. These control signals can be divided into three groups, which are as follows: 1) Visual Evoked signals 2) Spontaneous signals, 3) Hybrid signals.

Visual Evoked Signals (VEP) are the signals that an individual produces unintentionally in response to external visual stimuli. The Steady State Evoked Potentials (SSEP) and P300 are the two most well-known visual evoked signals. Visual evoked signals are dependent on external stimulation, which the individual may find awkward, taxing, or uncomfortable (Ramadan & Vasilakos, 2017).

When a subject experiences a periodic stimulus, such as a flickering image or modulated music, or even when the subject feels some vibrations, SSEP signals are produced in the brain (Lim et al., 2013) (Bera, 2015). In general, the brain reacts when a person experiences a certain change at a specific frequency. In other words, the brain's EEG signal intensity will rise to match the input frequency. Thus, signals in various brain locations are seen dependent on the sensory process.

There are many different SSEP signal types that can be identified, including steady-state visual potentials (SSVEPs), somatosensory SSEP, and auditory SSEP. SSVEP is frequently employed in a variety of applications. Typically, recurrent visual stimuli trigger SSVEPs signals. The visual cortex responds to visual stimuli like flickering images by generating SSVEP at a frequency that matches the flashing image (often between 6 and 30 Hz) (Bin et al., 2009) (Yin et al., 2009).

Time modulated VEP (t-VEP) BCIs, frequency modulated VEP (f-VEP) BCIs, and pseudorandom code modulated VEP are additional classifications for SSVEP based on the kind of modulation (c-VEP) (Ramadan & Vasilakos, 2017).

When the participant is exposed to an unusual or surprise task, an EEG signal that lasts for roughly 300 ms appears, known as P300. The "odd-ball" paradigm, in which the user is asked to pay attention to a random sequence of stimuli with one

stimulus occurring less frequently than the others, is typically used to generate this signal (Polich, 2007).

The P300 EEG waves are activated when this unusual stimulus is pertinent to the person. The P300 does not require any subject training; however, it does require repetitive stimulation, which could cause the subject to become tired and inconsistent.

Signals produced by a patient willingly and independent of external stimulus are referred to as spontaneous signals. The motor and sensorimotor rhythms, Slow Cortical Potentials (SCP), and non-motor cognitive tasks are the most well-known spontaneous signals.

Rhythms associated with motor activities, such as moving the arms, are referred to as motor and sensorimotor rhythms (Golub et al., 2016). These rhythms, with frequency bands at 8–13 Hz (μ rhythms) and 13–30 Hz (β rhythms), originate from the brain. The person may regulate the amplitude of these rhythms. Through extensive training, the subject is able to intentionally alter the amplitude of his or her sensorimotor rhythms. Motor imagery is the main technique used to control these sensorimotor cycles.

Motor imaging is the process through which the subject's motor intention is converted into control signals. For instance, the left-hand movement may produce EEG signals that are accompanied by decreases in the 8–12 Hz and 18–26 Hz rhythms in a particular motor cortex region (Lotze & Halsband, 2006).

Different applications could be used according to the motor imagery rhythms such as controlling a mouse or playing a computer game; it is always better to have a training period before using the motor imagery systems.

SCP is an EEG signal that falls below 1 Hz in frequency (Kim et al., 2004). It is a low frequency potential that has been seen in the frontal and central regions of the brain. The upper cortical dendrites' shifting depolarization levels are the cause of this potential. SCP is a very slow change in cerebral activity, either positive or negative, that can last anywhere from a few milliseconds and many seconds. The subject can control the creation of such signals, long-term training may therefore be even more necessary than it is for motor rhythms.

Many researchers no longer utilize SCP and instead prefer motor and sensory rhythms. (Ramadan & Vasilakos, 2017).

Cognitive tasks that do not include movement are those that power the BCI. Numerous activities are possible to complete, including musical imagination, visual counting, mental rotation, and mathematical computation (Dobrea & Dobrea, 2009).

Hybrid signals refer to different evoked or spontaneous signals produced simultaneously by the brain that are combined to provide control. As a result, a mixture of signals is used in the BCI system rather of just one type of signal being measured and utilised. The reliability and avoidance of each signal type's drawbacks are the key drivers behind using two or more types of brain signals as input to a BCI system (Amiri et al., 2013).

1.1.4 BCI limitations

Despite being a very useful tool for the improvement of people who have neuromuscular injuries and neurodegenerative disorders, the BCI has some limitations and inconsistencies.

The amount of training necessary for a subject to become proficient with the system is one of the biggest obstacles facing BCI. Most paradigms have lengthy training sessions, which might generate weariness in participants. Although there are cases of long-term usage of stimulus-based BCI (Sellers et al., 2010) (Holz et al., 2015), overall external stimulus paradigms such as P300-based systems may produce fatigue over lengthy durations of time. Additionally, it may be necessary for BCI researchers to gather calibration data at the start of each session due to subject dependence and even inter-session variability. A generic BCI model with zero training has been developed in several recent works using techniques like transfer learning to address this issue (Borhani et al., 2017) (Wang et al., 2015); these models proved to be inefficient compared to the BCI results obtained after a training period.

Many various decoding approaches, signal processing algorithms (Bashashati et al., 2007), and classification algorithms (Lotte et al., 2007) have been recently researched. However, the signal-to-noise ratio of the data derived from EEG signals is insufficient to control a system with multiple degrees of freedom, such as a neuro-prosthetic arm. In order to be able to properly control this system, more reliable, accurate, and quick online algorithms are needed. Recent years have seen several academics propose that active data selection and source localisation of EEG can

enhance classification ability (Abiri et al., 2019). Advanced machine learning and deep learning techniques may be used, according to suggestions made by other researchers (Längkvist et al., 2014) (Schmidhuber, 2015). These techniques have the ability to extract more features that can enhance categorization.

In the meantime, a specific standardization framework is required to assess how well decoding algorithms perform in particular applications and BCI systems (Dal Seno et al., 2010).

Scalp EEG has the potential to be marketed for the general population because it is seen as a cheap and low-cost brain monitoring technique (Nicolas-Alonso & Gomez-Gil, 2012). There are researches that assess behavioural changes with applicability to drowsy driving, in order to evaluate alertness/drowsiness from brain dynamics. Using a portable EEG headset makes it easier to comprehend the brain dynamics that underlie how the brain integrates perceptual functions in various situations. According to certain researches, there are connections between brainwaves and other sensory inputs, such as haptic feedback, and behavioural changes in reaction to auditory signals in a driving situation (Abiri et al., 2019). Many researchers have looked towards the creation of wearable and wireless EEG headsets as part of the technology's development (Malechka et al., 2015) (Suresh et al., 2015).

Additionally, dry EEG sensors have improved (Saab et al., 2011) (Zander et al., 2011). These sensors do not require skin preparation or gel applications that are required of conventional wet sensors. The advancement of these new EEG headsets may make BCI applications more widespread than they are now. For instance, a sleep management system that can rate the quality of sleep can be built on a forehead EEG-based BCI. The device could also be utilized as a depression treatment screening system that could test and predict the efficacy of fast antidepressant drugs. The technology of dry electrodes still has several drawbacks, though. For instance, the sensors hurt the scalp and are extremely sensitive to movement and muscle distortions. Additionally, the recording quality of modern dry headsets typically deteriorates after about an hour (Abiri et al., 2019).

The real-life applications in BCI are another difficulty. In other words, there are various challenges that need to be resolved in order to advance the research and the BCI applications from the labs to the practical applications. For instance, the cost of the BCI hardware and software is crucial in the development of efficient

applications since it encourages participation from more organizations and researchers.

It is anticipated that real-world applications would advance quickly with mobile platforms, which include both hardware and software. Examples of such mobile platforms include wireless EEG amplifiers and dry electrodes (Grozea et al., 2011) (Diez et al., 2011) (Chi et al., 2012).

The momentary inability to maintain peak cognitive performance is directly connected to fatigue. It's critical to reduce these fatigues if we want the system to continue to be useful. Optimizing the physical characteristics of the stimulus, for instance, using different types of stimulus patterns like high-frequency stimulus (Diez et al., 2011), high duty-cycle stimulus (Lee et al., 2011), and image-based stimulus (Bakardjian et al., 2011), might reduce tiredness. The use of an asynchronous system design enables the subject to interact with the BCI system at its own pace and comfort level. Such systems are difficult to design, and even just recognizing idle states can be difficult. By showing the subject a button to activate or deactivate the stimuli, some systems attempt to ease this problem (Venthur et al., 2010) (Pfurtscheller et al., 2010) (Figure 1.2).

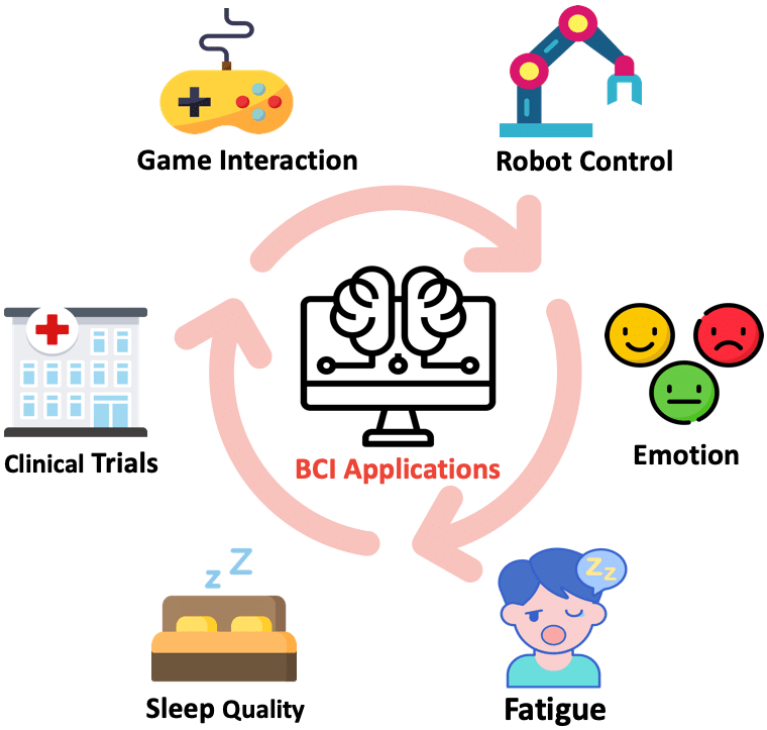

Figure 1.2 BCI applications

1.1.5 BCI for Error-related potential detection

Neurophysiological signals connected to error processing are called error-related potentials (ErrPs) (Ferrez & del R Millan, 2008). They are produced when incorrect actions are perceived and have been documented in numerous contexts over the past three decades, including when subjects perceive that they have made an error and immediately recognize it in choice reaction time paradigms ("response ErrP"), when they receive feedback from a prior choice without knowing whether it was correct ("feedback ErrP"), when they witness the errors of another person or an intelligent agent ("observation ErrP"), or when they use a Brain-Computer Interface (BCI) and receive a feedback that is unexpected ("interaction ErrP") (Kumar et al., 2019).

A midfrontal Error Negativity (Ne), also known as Error-related Negativity (ERN), which appears after errors have been made, is characteristic of ErrPs. This negativity is followed by a centro-parietal Positive deflection (Pe), which reflects conscious knowledge of error (Kumar et al., 2019) (Figure 1.3). Furthermore, it has been noted that right trials also produce a wave that resembles error negativity known as correct-related negativity (CRN or Nc). Studies using functional magnetic resonance imaging (fMRI) reveal that the anterior cingulate cortex is the origin of ERN and CRN (ACC) (Mathalon et al., 2003) (Pires et al., 2022).

The elements of an ErrP are naturally elicited in the brain within a time window of 500 ms (Kumar et al., 2019). Thus, there are numerous real-time applications for its automatic detection.

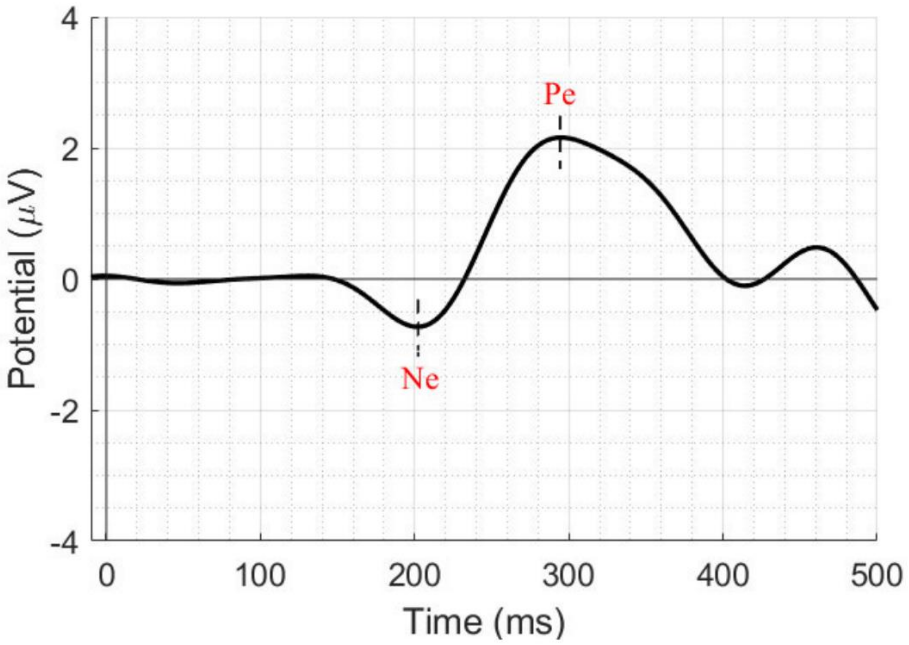

Figure 1.3 ErrP waveform

The possibility of automatic error signal identification by machine learning can be important for many real-life applications in clinical and non-clinical contexts given the importance of error monitoring in social interaction, behaviour, human-machine interface, and cognitive learning. As a proof-of-concept, ErrPs have already been used in a number of applications, including the detection and correction of BCI decisions to improve reliability, the adaptation of BCI systems over time, and the learning of artificially intelligent systems (Kumar et al., 2019).

The BCI community has recently become quite interested in the idea of employing ErrPs as a reward to train or adapt intelligent systems via reinforcement learning. ErrPs are utilized as a reward in reinforcement learning-based settings (Chavarriaga & Millan, 2010) (Xavier Fidêncio et al., 2022) (Figure 1.4).

Asynchronous detection in continuous tasks, low accuracy of single-trial detection, calibration requirements, and low generalization across applications/tasks/subjects are just a few of the difficulties that must be overcome to fully utilize error recognition, despite the remarkable and successful use of ErrPs and other error-related neural signatures. These difficulties have forced the usage of automatic error

recognition, mostly in highly controlled (and occasionally irrational) applications and scenarios (Pires et al., 2022).

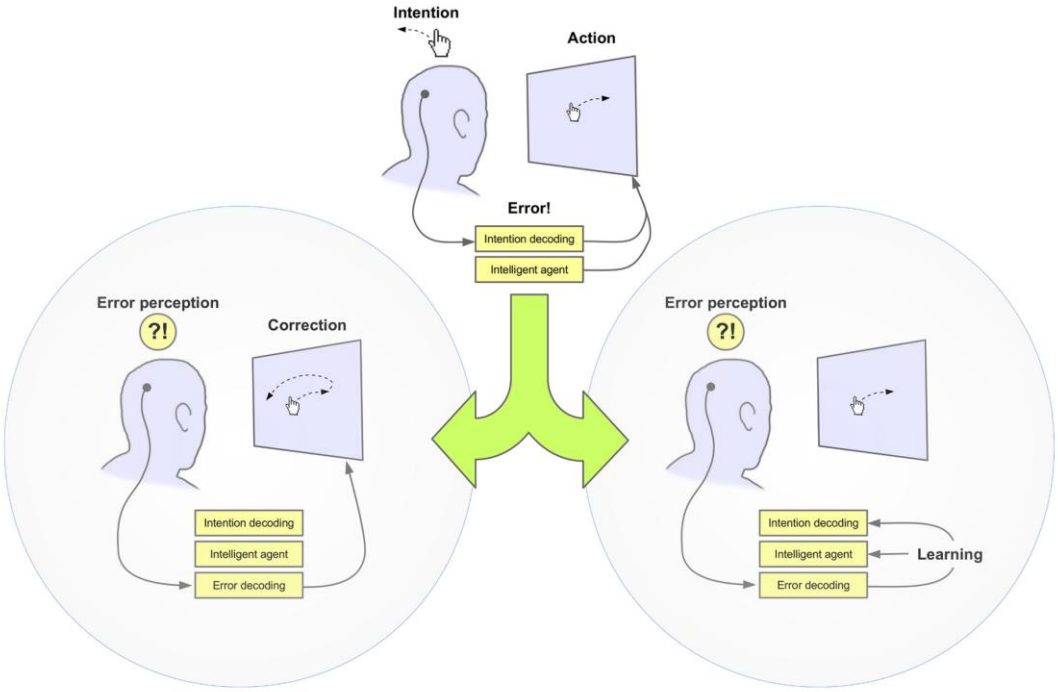

Figure 1.4 ErrP for reinforcement learning

Finding the disparity between the observed action and the translated action in the BCI platform is one method of getting the ErrP (Abiri et al., 2019). The interaction between individual and the BCI system was analysed form Ferrez and Millan (Ferrez & del R Millan, 2008). After feedback, they noticed positive peaks at 250 milliseconds and negative peaks at 320 milliseconds. Additionally, they noticed that as the error rate falls, ErrP amplitude increases. The effects of a subject watching over an outside agent that the subject cannot control were examined by Chavarriaga and Millan. They classified the EEG signal using a Gaussian classifier employing a cursor movement paradigm to get the posterior probability of moving the cursor incorrectly (Chavarriaga & Millan, 2010).

It was discovered that the ErrP response was most closely linked with electrode positions Fz, FCz, and Cz (Iturrate et al., 2011) (Mousavi & de Sa, 2019). In a research by Itturate et al., participants watched a virtual robot complete a reaching activity. The subject was told to evaluate the robot's movements based on knowledge of the proper course. Calculations of the averaged EEG waveforms at each electrode position revealed a sizable difference between the robot's correct and

erroneous performance. On error trials, a sharp positive peak was seen at around 300 ms, followed by a sharp negative peak at around 400 ms (Iturrate et al., 2010b).

1.1.6 ErrP application with the BCI system

The scientific community developed a lot of ErrP-based BCI in order to help people with motor impairment (Kumar et al., 2019); some of the main application field is described as follows.

Robots have a lot of potential for helping persons with motor disabilities get better and living a better life. The incorporation of ErrP-based correction mechanisms in robot control has been the subject of extensive prior research (Figure 1.5). According to Iturrate et al., when a group of four healthy volunteers saw an actual robot operate, the brain's error-detection mechanism was activated (Iturrate et al., 2010). The experiment involved seeing a robotic arm with five degrees of freedom (DOF) conduct reaching tasks correctly or incorrectly to five specified positions. In classifying the ErrP signal, the researchers report average sensitivity and specificity of 78.97% and 82.58%, respectively. This suggests the possibility of error detection and correct robotic behaviours in a single trial. An ErrP signal was employed as feedback in a different intriguing work that used a shared-control technique to control a robot in a genuine 2D movement challenge. By exploiting the ERN and CRN signals, the robot accomplished the participant-selected goal without any prior training in less than 120 seconds (Iturrate et al., 2013). Similar tactics were employed by Penaloza et al. in a navigation project, and they reported an ERN classification rate as high as 82%. They used the ERN signal as an emergency signal to stop the robot's navigation owing to any perceived hazard (Penaloza et al., 2015). In order to enhance the performance of a robot conducting a binary choice task, Salazar-Gomez et al. described how a secondary ErrP signal can be produced when the system incorrectly classifies the ERN signal as the CRN and vice versa. They also stated that implementing the secondary ErrP method can improve the classification performance of the system by over 20%, based on an offline analysis. The reported secondary ErrP signal was easier to categorize and had more robust properties than the primary ErrP signal (Salazar-Gomez et al., 2017).

The majority of our attention has been on robotic control, where the participant's duty was to passively monitor the robot's behaviour while the robot used the ErrP signal as feedback to perform or accomplish the intended goal.

Now it will be described about robot active control. In their study, Bhattacharyya et al. used the sensorimotor rhythm (SMR), P300, and ErrP EEG signals to positionally manipulate a robotic arm to achieve a goal (Bhattacharyya et al., 2014). The arm was aligned with the target and any misclassified motor imagery (MI) actions were undone using ErrP. The authors reported that the average reaction time was one second. Once a robotic connection has been chosen via MI, it moves continuously in the chosen direction up until ERN is elicited. Participants would have to wait for the required connection to become active before attempting to control it since the links follow a specified order of activation. Because of this, it will take longer to get to the desired "target position," making the sequential control of the robotic linkages a flaw or downside of these research (Bhattacharyya et al., 2017). Additional research has confirmed the viability of employing ErrP for robotic control. In the object selection task, Ehrlich and Cheng used an ErrP signal to co-adapt a robot's gaze behaviour pattern (Ehrlich & Cheng, 2018). In this activity, a user attempted to predict the object that the robot would select based on its gaze patterns. Through the use of this method, the accuracy of proper behaviour assessment of the robot grew from the initial chance-level (33%) to 70-90% within 10–40 trials. None of the research that were presented tested their methodology on people who had motor impairments.

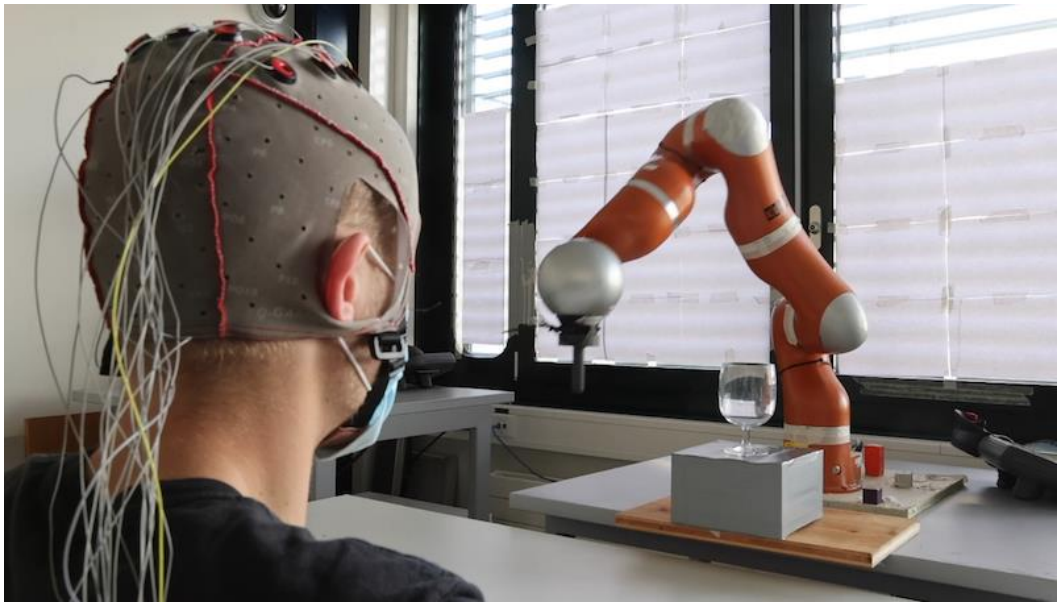

Figure 1.5 ErrP acquisition for robot control

The ErrP signal has been widely used as a correction mechanism in P300 based BCI-spellers (Figure 1.6). In these spellers, on the detection of the ErrP, the system can cancel the currently selected character and select the character with the second-highest probability instead. Dal Seno et al. demonstrated the use of the ErrP signal in P300 spellers with two participants (Dal Seno et al., 2010). However, in this study, the use of the ErrP in a speller showed little to no improvement. A major problem in their experiment was the low ErrP classification accuracy that may have led to the poor performance of the speller. Schmidt et al. assessed the improvement of the speller performance with the incorporation of ErrP. With twelve participants, they reported an increase of 49% in the spelling speed compared to the case without the ErrP (Schmidt et al., 2012). The studies undertaken so far were focused on and included healthy participants only. In 2012, Spuler et al. conducted experiments with six severely motor-impaired subjects along with eight age-matched healthy participants. A performance improvement of 0.37 bits/trial in the motor-impaired subjects and 0.73 bits/trial in the age-matched healthy participants was observed (Spüler et al., 2012). It is worth mentioning here that Spuler et al. reported similar ErrP patterns in the motor-impaired participants and healthy counterparts, which supports the use of the error correction mechanism in BCI spellers for disabled people as well. Whereas the approaches so far employed the ErrP signal for deletion of the wrong character, a natural progression would be to implement the automatic error correction.

Figure 1.6 P300 based BCI-spellers

People with physical disabilities can utilize wheelchairs as a mobility assistance; the control of the wheelchair can be directly connected to a BCI system (Figure 1.7). Brain-controlled wheelchairs (BCW) have been operated using a variety of different brain signals, including P300, SSVEP, SMR, and muscle potentials (Fernández-Rodríguez et al., 2016). Because BCW, like other BCI applications, is prone to errors in discerning human intent, the ErrP signal can be used to improve BCW's performance. Perrin et al. proposed using error-potentials in a brain-controlled semi-automatic wheelchair system (Perrin et al., 2010). To test the viability of the ErrP usage in this application, they ran an experiment in which participants saw a robotic wheelchair navigate in both a realistic simulation and a real-world setting. According to sources, if the semi-automatic wheelchair made a mistake that prohibited it from completing a task, the ErrP would be triggered. Taeb et al. further confirmed the ErrP signal's presence using ten healthy volunteers in a brain-activated wheelchair experiment(Taeb et al., 2014). The ErrP signal was triggered as a result of feedback that suggested the BCI system had given a false response.

This thesis focuses the attention on the improvement of this last particular field of research.

Figure 1.7 ErrP acquisition for wheelchair control

1.2 Motivation and objectives

The state of the art emphasizes that it is possible to navigate the wheelchair using only brain signals, but this system does not guarantee autonomous and safe navigation due to the restriction applied during the experiment analysed, effectively limiting its applicability to a laboratory environment for further experimentation. Currently, such a system is still considered to be in a primitive state and needs to be further inspected.

In order to supply the wheelchair with a security system that maintains the efficiency and accuracy at high levels, it is important to create a protocol for correcting the predictive algorithm of brain signals. Based on the previous studies of the ErrP, this system is hypothetically implementable. According to this hypothesis, the wheelchair would be able to navigate safely by converting specific EEG signals into command for the navigation system of the wheelchair.

This algorithm should dynamically evaluate the brain response during the implementation of a navigational command and if the person experience an unexpected outcome, the brain generate a clear ErrP response form the frontal-central area and with the information gathered from the ErrP thus generate the wheelchair corrects the trajectory and resumes the correct path.

The objective of this thesis therefore focuses on determining whether there is evidence of error-related potentials generated during the movement of the wheelchair under controlled circumstances; if there is any evidence of error-related potentials under these conditions, we will test the effectiveness of classifying this signal to create a baseline for the implementation of the future full correction algorithm during wheelchair navigation.

2. Methods

2.1 Participants

Ten healthy participants were recruited for this experiment, five male subjects and five female subjects who voluntarily participated in the experiment. All participants in the study were between the ages of 20 and 40 years old (mean age 25±5.3) In order to participate, every individual in the experiment had to fill out a consent form that detailed all the information needed, the parameters derived from the experiment, how they were utilized, the experiment's measurement procedures, the advantages of this study, potential drawbacks, and potential hazards.

Each person has given their permission for the processing of personal data for the purposes of completing this research project after being made aware of all the aforementioned information. Furthermore, none of the subjects had any diseases or were undergoing any kind of treatment at the time the brain signals were being gathered. Each subject was asked to participate in one measurement session, during which all extrapolated brain data required for the study's successful continuation were obtained.

2.2 Materials

2.2.1 Wheelchair

For this experiment was employed the motorized wheelchair produced from the company “Vassili” under the name of “motorized wheelchair HI-LO VARIO” (Figure 2.1).

This device is developed in order to help people who suffers of severe motor disabilities when performing daily tasks; specifically this device has two motorized wheels (which are located to the front of the vehicle) and two free wheels (which are located to the back of the vehicle), the navigation with this wheelchair is managed by the person using a joystick integrated into the wheelchair's armrest that allows the person to freely control the 360° movement of the medium holding up to 120kg with a maximum speed of 10 km/h.

In the case of this experiment, the navigation function of the joystick has been replaced by a remote control with a gamepad that has been adapted in line with the needs of the study to be carried out.

Figure 2.1 motorized wheelchair HI-LO VARIO

2.2.2 Gamepad

Specifically, the gamepad employed for this operation is a common tool widely used; it is the "wireless gamepad Logitech F710" (Figure 2.2); the gamepad was connected to the computer and, with a customized program, it was possible to control the wheelchair's linear and angular movement: specifically, with the right analog stick of the gamepad was possible to control in a continuous way the entire navigation system of the wheelchair while it was also possible to control in a discrete way the wheelchair using specific buttons that altered for a predetermined amount of time the navigational properties.

Figure 2.2 wireless gamepad Logitech F710

2.2.3 EEG system

A eego™sports (AntNeuro, Netherlands) helmet has been used for the acquisition of EEG signals (Figure 2.3): it is a device for the acquisition of 64 electrodes positioned according to the standard 10-20 layout: according to this scheme the standard configuration set the position of the basic electrodes around the scalp based on the percentage of the circumferential measure of the skull, specifically, the electrode must be positioned at 10/20% from each other depending on their position (Seeck et al., 2017) (Figure 2.4). The helmet must be positioned properly in order to correctly acquire the brain signals. Although the helmet's acquisition capacity allowed for the use of 64 electrodes, it was decided to use only 32 during the experiment because the fronto-central region is the only part of the brain that was of interest, making it unnecessary to integrate measurements on other peripheral regions like the occipital one, which results in a faster setup time of the helmet during the experiment; the electrodes thus used for this experiment were Fp1, Fp2, F1, F2, Fz, Fc1, Fc2, Fc3, Fc4, Fc5, Fc6, Fcz, C1, C2, C3, C4, C5, C6, Cz, Cp1, Cp2, Cp3, Cp4, Cp5, Cp6, P1, P2, P3, P4, P5, P6, Pz (Seeck et al., 2017). In order to enhance the low voltage intensity signal acquired from the helmet a AntNeuro EEG amplifier (Figure 2.5) was adopted; the connection between helmet and amplifier was performed using shielded cables that cleared the signal by eliminating the electromagnetic interference created form the wheelchair motors.

Figure 2.3 eego™sports helmet

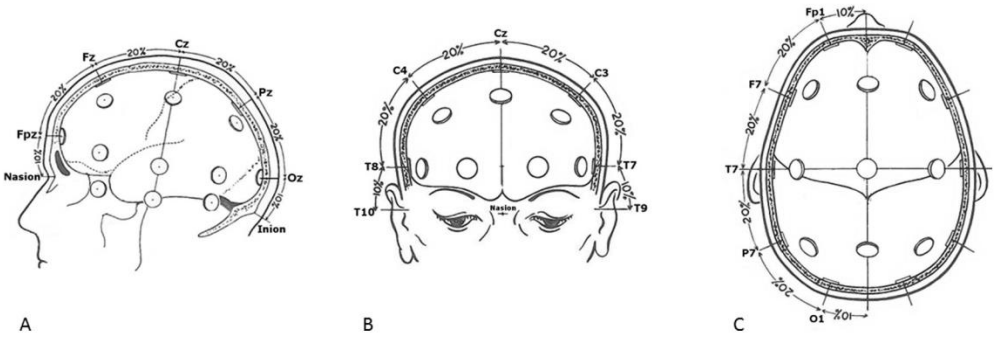

Figure 2.4 standard 10-20 layout

Figure 2.5 AntNeuro EEG amplifier

2.2.4 ROS-Neuro

In order to enable the control of the wheelchair with the gamepad instead of the joystick integrated into the wheelchair's armrest, a custom program was developed using the Robot Operating System (ROS) programming libraries to control the wheelchair's navigation system; ROS is not a proper operating system (OS) but it is a open source middleware for the creation of robot software. As such, it offers services for a heterogeneous computer cluster, including hardware abstraction, low-level device control, implementation of frequently used functionality, message-passing between processes, and package management (Quigley et al., 2010).

The program developed was integrated into a “launcher file” that has three main functionalities which all happened simultaneously when the program is launched on the computer; this specific file is used to execute multiple codes (referred as ROS “nodes”). Specifically, this launcher is responsible for the brain signal

acquisition, the gamepad input acquisition, and the conversion of the gamepad input into specific commands for the wheelchair.

First, the launcher enables the EEG helmet to acquire 32-channel EEG data from the skull of the person at sample rate of 512Hz. The data thus acquired are stored in the computer for further evaluation.

The second main functionality is represented by the node called “joy”; this node is used in order to properly acquire the input from the gamepad sorted in two classes: buttons and axes (*Joy - ROS Wiki*, 2022). Using this node, it was possible to use the gamepad to drive the wheelchair. Inputs gathered form the joy node were employed in a custom program.

The third and final functionality of the launcher file is represented by the custom code for the navigation of the wheelchair with the gamepad.

Five different functions have been associated with five different gamepad buttons: specifically the user had access to the Start button (set at the A button), the Stop button (set at the B button), the button to turn Right (set at button R1), the button to turn Left (set at button L1) and finally the special button Emergency (a special button that could only use the supervisor set at the X button). Every time the user requests a command the code checks the lists buttons and axes generated by the node joy and verify the type of information contained; if one of the buttons set for the movement of the wheelchair changes its value the code checks which task should be performed and communicates the operation directly to the navigation system of the wheelchair.

The main goal of the program was to create a direct connection between the gamepad and the navigation system of the wheelchair. The code also had a special property; in fact, while communicating with the wheelchair navigation system, some commands are randomly reversed; this kind of function has been designed to induce the user to generate a ErrP caused by the wheelchair's unexpected implementation of a command. After this inversion, the system returned to its original state to allow the person to correct the trajectory. The error rate was 25% as a standard condition; this percentage was chosen to ensure a high frequency of command inversions without accustoming the user; in fact, if the person anticipates a wrong rotation, the type of response produced by the affected brain area changes and loses its statistical validity.

Only the rotational commands were randomly inverted by the code while the control of the linear movement of the wheelchair was unchanged throughout the whole experiment.
As a result, in the event of an impending collision with an object caused by an inverse rotation during a curve in the route, it was always possible to stop with the greatest degree of safety without endangering the user or the working equipment.
An additional functionality was added to the launch file for this experiment; this final addiction was responsible for the control of the odometry; the odometry it is a system responsible for assessing the position of the device relative to the starting point throughout the measurement period. From the odometry it was possible to derive useful parameters such as the acceleration profile and rotation speed in the various directions in each temporal moment.

2.3 Experimental protocol

The entire experiment was conducted in the university's laboratory "IasLab - Intelligent Autonomous System Laboratory". The operator was responsible for the correct placement of the EEG helmet on the participant skull; a water-based gel and ions have been used to ensure better conduction between the scalp and the helmet detection site to measure the signals generated; this step is necessary to avoid hair from creating measurement noise patterns during the wheelchair session.
A continuous signal was acquired for each measurement session (referred to as a run); overall eight runs were recorded for each subject. Each signal was stored in a file that contains information about all the electrodes as well as the relative odometry.
Each subject had to follow the predetermined track using the custom controls in order to finish the measurement accurately. Eight checkpoints (CPs) were included in the path, two of which were related to the starting point and the destination and six of which were intermediate. For a run to be declared valid, the wheelchair had to pass through each CP using all four wheels.
The path was designed to force the user to perform as many turns as possible in order to have more opportunities for the random command inversion that would lead to the generation of an ErrP (Figure 2.6).

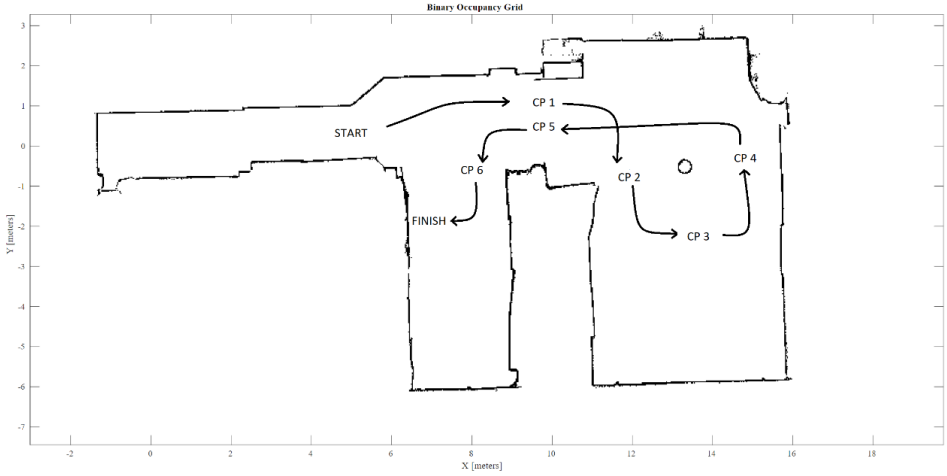

Figure 2.6 Experimental track

The route was then divided according to the following scheme: after a first linear stretch towards CP 1 the user had to make a series of curves first to the right and then to the left to complete a complete a full turn around a column of the laboratory through the CP 2-4, then follow a second linear stretch towards CP 5 and then make two quick curves to the left, to cross CP 6, and finally to the right to reach the finish line.

Pressing the Start button allowed the wheelchair to acquire a constant linear speed, which was maintained over time regardless of which rotational commands were inserted as input. The button on the Stop function allowed the chair to stop its movement by setting the constant linear speed to 0 km/h.

As for the rotational buttons, both the rotation to the right and the rotation to the left, were characterized by a special operation; in fact, the rotational control was done in a discrete way, which means that, at the moment when the user pressed the command to rotate the wheelchair, for each button pressed the wheelchair performed a rotation for a standard time in the desired direction; specifically each command generated a rotation for a predetermined amount of seconds in the desired direction at the constant speed; therefore, in order to perform a wider rotation it was necessary to execute several commands of the same time in succession.

Last, the special function Emergency was used to disable any other functions while also enabling the continuous, error-free control of the wheelchair using the right analog stick at a constant speed; this specific function is implemented in order to

correct the trajectory of the wheelchair whenever the user goes off track; the operator is then able to bring the wheelchair back to the right position.

The value of the linear and angular velocity was set at 0.8 km/h while the rotational time was set at 1.5 seconds.

During the measurement session each user was instructed to fixate a cross displayed on a small monitor in the front in order to limit as much as possible the measurement noise due to eye movements. Furthermore, the user was instructed not to blink during rotation input for the same purpose; this required the user to use his peripheral vision to navigate on the wheelchair. A screening period of around 20 command input (referred to as a "trial") was given to every subject in order to get familiar with the task. Due to the limited perception of the route, the experiment was closely supervised by the operator that was always ready to instruct the person to stop if any kind of issues arose.

When the subject encountered an obstacle, the operator was responsible for instructing the subject to stop using the Stop feature. After instructing the subject to stop, the operator had to press the special Emergency button in order to move the wheelchair back into the proper position so that the measurement could proceed. When the wheelchair returns on the correct path towards the completion of the measurement the operator allows the person to use the Start feature to continue the measurement session.

Each subject had to follow the course eight times over the entire measurement period to guarantee enough recorded data. The length of each single run, which varied depending on the subject's wheelchair-navigation skills and the frequency of incorrect orders that caused the wheelchair to deviate from the intended trajectory, was on average 5±1 minutes. The entire session, including the time to fix the EEG helmet, the time to set up the associated equipment and the interim break for the user to unwind, had to be finished within an hour.

2.4 Data analysis

We investigated whether it is possible to identify EEG patterns that are related to the ErrP generation. In order to achieve this, we examined the elicited EEG patterns on the software MATLAB and investigated the possibility of recognising the ErrP pattern from a single-trial analysis.

First, EEG signals were band-pass filtered at [1, 12] Hz with a casual 4^{th} order of Butterworth filter; then, they were filtered again with a common technique useful for removing artifacts known as “Common Average Reference” (CAR) which reduces the fundamental measurement noise by removing the average EEG value from every single electrode (Alhaddad, 2022) (Ludwig et al., 2009).

For every command sent to the wheelchair, EEG signals were extracted within a time window of 1025 samples (corresponding to two seconds total) starting from 0.5 seconds before the command was delivered to the wheelchair up to 1.5 seconds after, thus defining a trial. This process allows to study the brain response to the outcome of the command on the wheelchair, along with the EEG signals acquired during the preparation to the execution of a command.

From this extraction 3 channels were specifically analysed out of the 32 total. The channels selected were Fz, Fcz and Cz; these channels analyse the responses generated by the brain surface in correspondence between the frontal and central part of the brain along the central line separating the head in two halves; these are the areas of greatest interest for the detection of error potentials (Ferrez & del R Millan, 2008) (Schalk et al., 2000).

We analysed two different classes of trial for every channel selected; these classes are related to the generation of a correct command or the generation of an incorrect command; then we computed a mean for each class, in order to understand the difference between the brain reaction during the execution of a correct command and the execution of an incorrect command throughout the two seconds analysed.

In addition, we chose to perform a topographic analysis of the entire surface of the brain in five specific instants in time; this analysis was carried over a small-time window that covered from 0.2 seconds prior to the command delivery up to 0.6 seconds after; the instants thus analysed were [-0.2 0.0 0.2 0.4 0.6] seconds relative to the command delivered.

This additional analysis was made to highlight the brain's behaviour during the most significant moments of each trial in accordance with the state of the art (Ferrez & del R Millan, 2008) (Schalk et al., 2000).

Two further aspects were considered afterwards; these traits were related to the rotation of the wheelchair, which led to additional analyses. The first analysis considered the delay generated during the implementation of the command on the

wheelchair: we tested the possibility of a delay generated from system before the command implementation, which could lead to a delayed response from the subject. For every trial, each window of acquisition was shifted in order to align the latencies of all peaks and obtain a clearer average signal. Specifically, we computed the max rotational value for each trial and shifted the original window to set the initial point of acquisition when the wheelchair reached 20% of the maximum rotational velocity.

The second aspect tested was relative to the different type of rotation: we verified the possibility that a concordant and discordant rotations could lead to a different response in each person. We divided the dataset in two classes and analysed them separately.

To perform this division, we employed the information acquired from the odometry: for every command implementation we verified if the previous command led to a rotation in the same direction (which results in a concordant trial) or in the opposite direction (which results in a discordant trial).

2.5 Data classifications

Following the filtering and subdivision of the EEG signal into different windows we proceeded to create a set of rules for the feature extraction.

A "feature" is a distinctive property of the signal that is capable to characterize each class of the signal. Through a direct comparison of the particular parameter taken into account between the different type of trials (i.e., correct rotational trial and incorrect rotational trial), features are assessed according to their discriminability; highly discriminating features lead to a more accurate distinction between the two signal types.

In order to determine which features were the most discriminating for the characterization of the type of signal, nine possible attributes of the signal that represent the most used parameters in related studies were tested to ensure greater accuracy in the classification process. Four of these features were relative to the maximum value of each trial, the minimum amplitude of each trial and their relative latency (Jrad & Congedo, 2012). The remaining five attributes correspond to the mean of the EEG amplitude within a different timespan of the original time window acquired; specifically, the original two-seconds time window was divided in five smaller time windows of 400ms each (Iturrate et al., 2011).

Among these attributes the most discriminant features for each person were evaluated using a scoring algorithm known as Fisher score, which is one of the most efficient statistical evaluation meter for the EEG analysis (Dong et al., 2016) (Lei Cao et al., 2010).

In order to apply this statistical test, we must define two classes that contain a specific type of trial using a priori information (i.e. correct rotational trail and incorrect rotational trial); following the class division the Fisher score can be applied in order to evaluate any potential feature; the test considers the mean and the variance of the chosen feature in both of the trial classes and compares them in order to produces a score. Being k the feature selected, μ the mean and σ the standard deviation for the two class *C1* and *C2*, the Fisher score is evaluated with the following equation:

$$FS(k) = \frac{abs(\mu_{C1}(k) - \mu_{C2}(k))}{\sqrt{\sigma^2_{C1}(k) + \sigma^2_{C2}(k)}}$$

A high fisher score is a sign that the parameter being evaluated is highly discriminating for the two classes. After each potential feature had been given a Fisher score, the most discriminating ones were assessed by exceeding a predefined threshold, which equates to half of the highest fisher score value recorded plus 20% of the same value. On this basis, it is possible to confirm which attributes, in fact, best capture the distinction between the two classes. At this point the features that exceed the selected threshold are selected and are used for the real classification.

The goal of the classification process is to create an algorithm based on the feature selected that can highlight the distinctive characteristics of brain signals corresponding to correct and incorrect rotations. Therefore, the classification algorithm must be able to identify with high precision whether the type of signal analysed correspond to a correct or incorrect command implementation without any a priori information.

We chose to adopt a cross-validation system called leave-one out (LOO) which is one of the most common cross-validation methods used (Cawley & Talbot, 2003); in each iteration we selected 7 runs for the training-set and 1 run for the test-set.

For every iteration we produced a linear model through the MATLAB function "fitcdiscr" based on the recorded values of features and the corresponding trial type; the model thus created was then tested on the remaining run (i.e., the test-set) and

on the training-set itself in order to evaluate the ability to correctly distinguish between different type of trial without a priori information.

Following the aforementioned scheme for the division between training-set and test-set, all runs were utilized as test sets once in the succeeding iterations, while the remaining measurements were used for the training set, for a total of eight iterations. Obtaining overall high accuracy, that is consistent across iterations suggests that the features obtained during the fisher score analysis were chosen correctly.

The overall accuracy has been evaluated using the MATLAB "perfcurve" function: this function calculates the ratio of false positives to false negatives and generates a curve called “ROC” (receiver operating curve); the perfect classifier is represented by a curve passing through the extreme point 0,1, while a classifier that classifies incorrectly 100% of the time is represented by a graph passing through the extreme point 1,0. This curve generate a parameter called AUC (area under curve), which represents the ability of the classifier to perform the binary composition correctly (Fan et al., 2006).

3. Results

3.1 Temporal analysis

Figure 3.1 shows the average between subjects ("grand average") for both correct rotational trial (i.e., "Correct" blue curve) and incorrect rotational trial (i.e., "ErrP" red curve) for the three channels of most interest Fz, Fcz and Cz; we chose to represent only 1 second out of the 2-seconds original time window; if fact for every subject we chose to evaluate the brain behaviour throughout the whole trial, while for the grand average we chose to focus only on the time spawn where the ErrP typically appears (Chavarriaga & Millan, 2010). The "Diff" black curve represents the difference between the mean of the EEG signals for the different type of trials: through a visual inspection of this curve, we can understand the brain's reaction to the different type of ErrP for each subject. The grand average highlights a positive peak followed by a negative deflection in the frontal-central area within the first 0.6 seconds from the command delivery, which is typical of the waveform of the ErrP, especially in the Fz channel (Iturrate et al., 2011) (Mousavi & de Sa, 2019). Because each subject's positive and negative peaks have a distinct delay due to the different brain behaviour, this curve is represented with a low amplitude. This low amplitude is also justified because some subject (e.g., subject 1 in the Fz channel, Figure 3.3) generated a clear ErrP that differentiate itself from the EEG pattern generated during a correct rotational command, while other subject (e.g., subject 5, Figure 3.5) generated an ErrP which is less easy to differentiate from the correct rotational trial EEG waveform. All subject results are reported in the Appendix 1.

Figure 3.2 depicts the average between subjects of the topographic map of the brain for correct rotation trial (displayed in the top row) and incorrect rotation trail (displayed in the bottom row) within a time window of 0.8 seconds, which starts from 0.2 seconds before the input registration up to 0.6 seconds after the rotation command is implemented. From this representation it is possible to observe the whole brain behaviour during specific instant of time: the presence of a red area indicates a positive peak while the blue area represents a negative peak. Similarly, to the temporal analysis of the Fz, Fcz and Cz channel (Figure 3.1), since the positive and the negative peaks have different latencies, the topographic value reported is low; nevertheless, it is possible to distinguish a positive peak in the frontal-central area of the brain during the interval 0.0-0.2 seconds after the input

delivery as well as a negative peak during the interval 0.4-0.6 seconds after the input delivery.

These results are clearer and easier to inspect visually in order to understand the difference between the brain's behaviour during the two types of trial: in fact, comparing the different response between trials, some subjects (e.g., subject 1, Figure 3.4) display a clear positive peak followed by a negative peak in the frontal-central area of the brain during the inspection of the ErrP related trial only. Conversely, the results for the other subject (e.g., subject 5, Figure 3.6) display little difference between the brain's behaviour for each type of trial: these results lead to a major difficult for the evaluation of the type of trial during the classification process, which generate an overall lower accuracy compared with the classification of the subject that showed a clear ErrP. All subject results are reported in the Appendix 2.

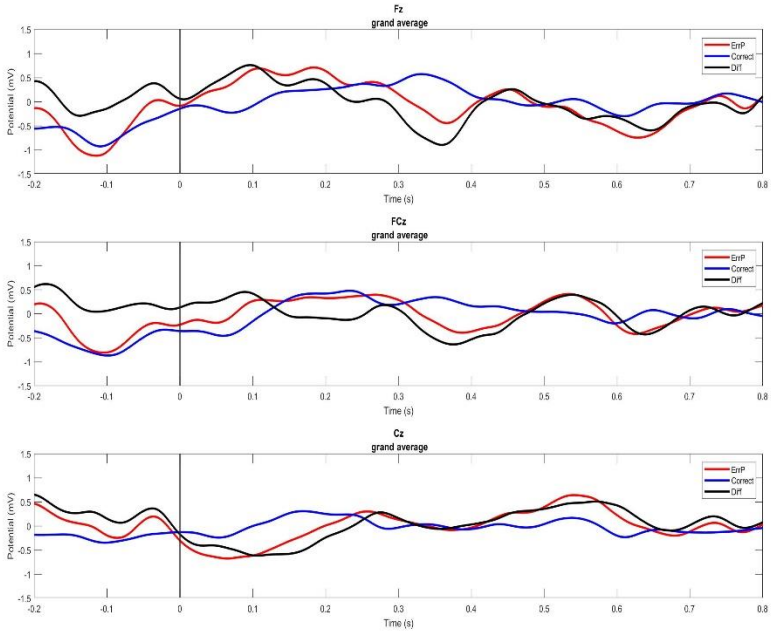

Figure 3.1 – Fz, Fcz and Cz Grand Average

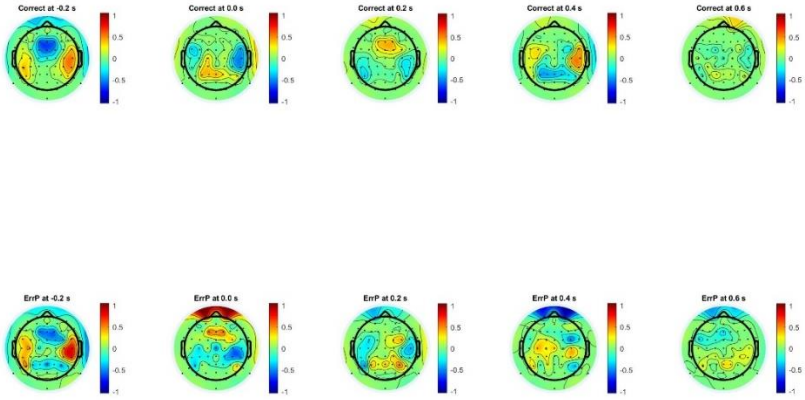

Figure 3.2 – Topographic Grand Average

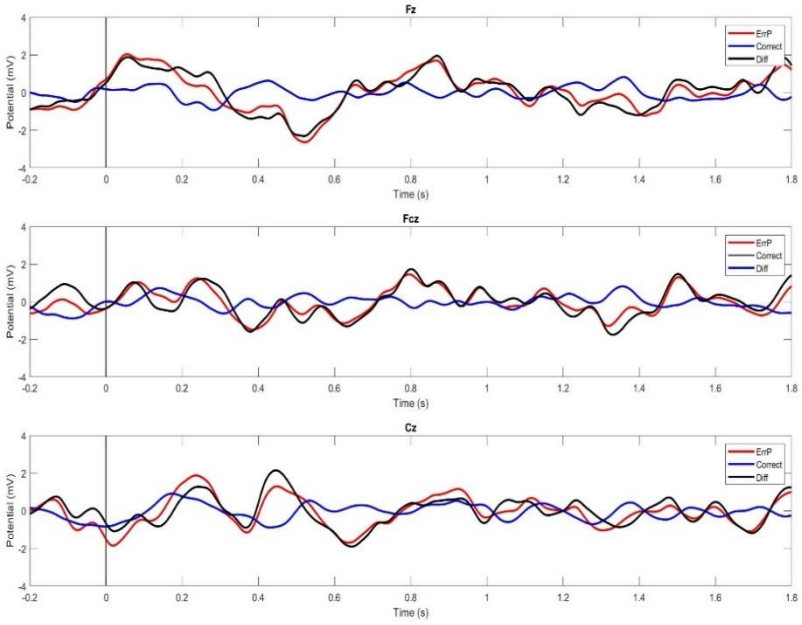

Figure 3.3 – Fz, Fcz and Cz of subject 1

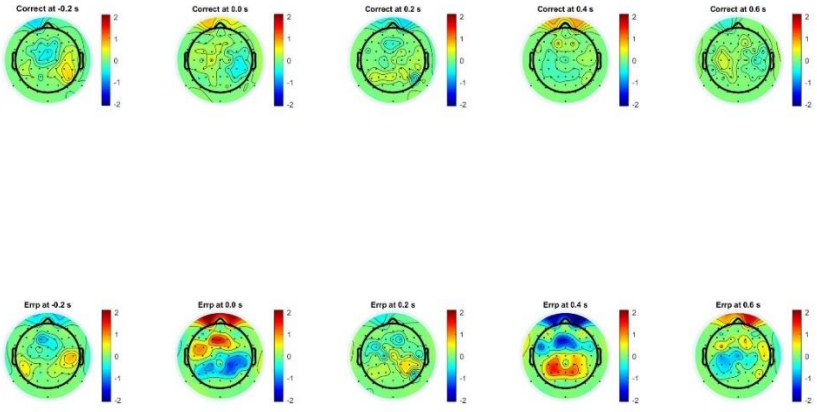

Figure 3.4 – Topographic view of subject 1

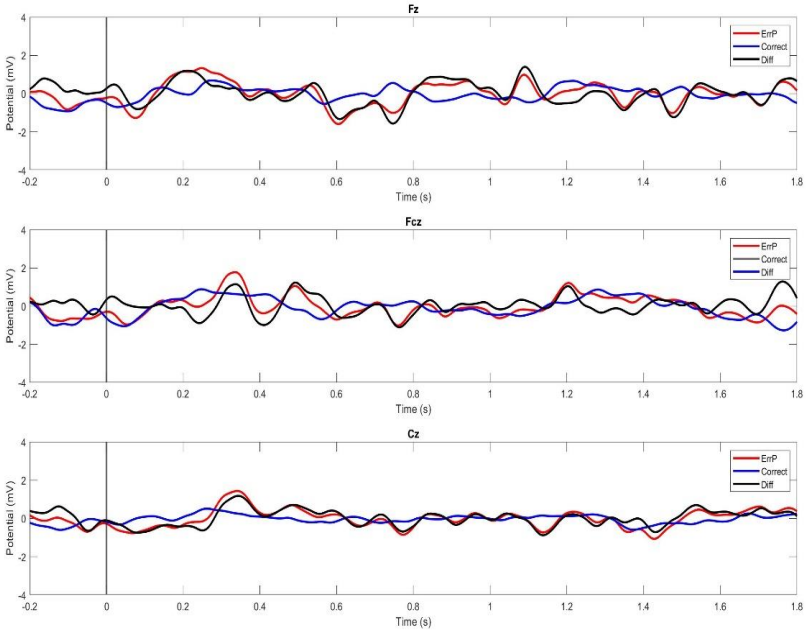

Figure 3.5 – Fz, Fcz and Cz of subject 5

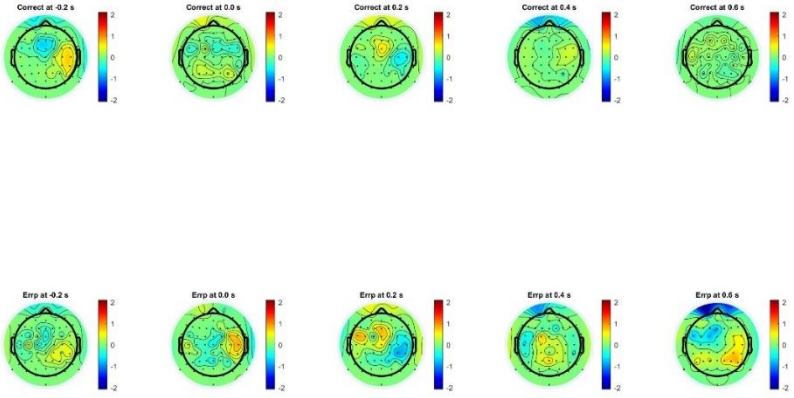

Figure 3.6 – Topographic view of subject 5

3.2 Classification results

In Figure 3.7 and Figure 3.8 are displayed the ROC curves produced form the leave-one out classification for the subject 1 and the subject 5, which are the users that generated respectively the clearest ErrP and the least visible ErrP. These results show the eight interactions of the LOO classification in which the classifier use seven runs to create a training set and one for the test-set; the overall accuracy is represented by the AUC parameter, which evaluate the overall area under the curve thus defined. All subject results are reported in the Appendix 3.

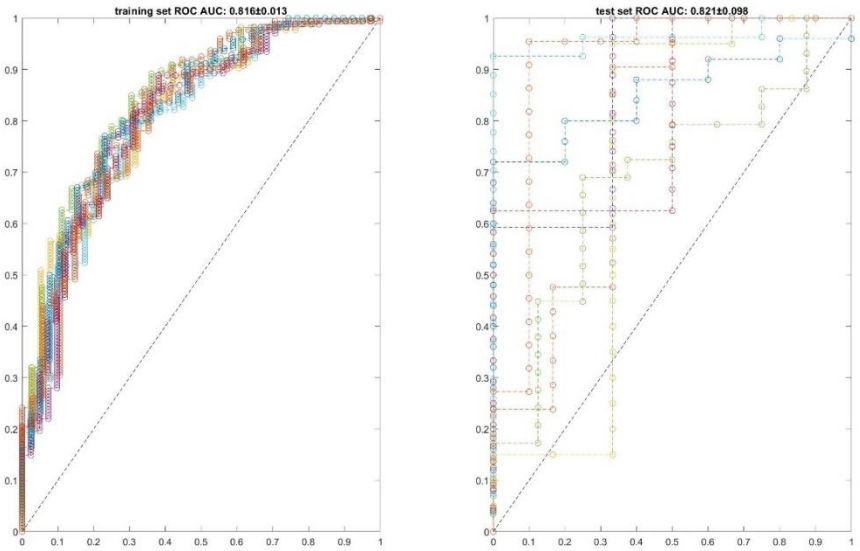

Figure 3.7 – ROC curve for subject 1

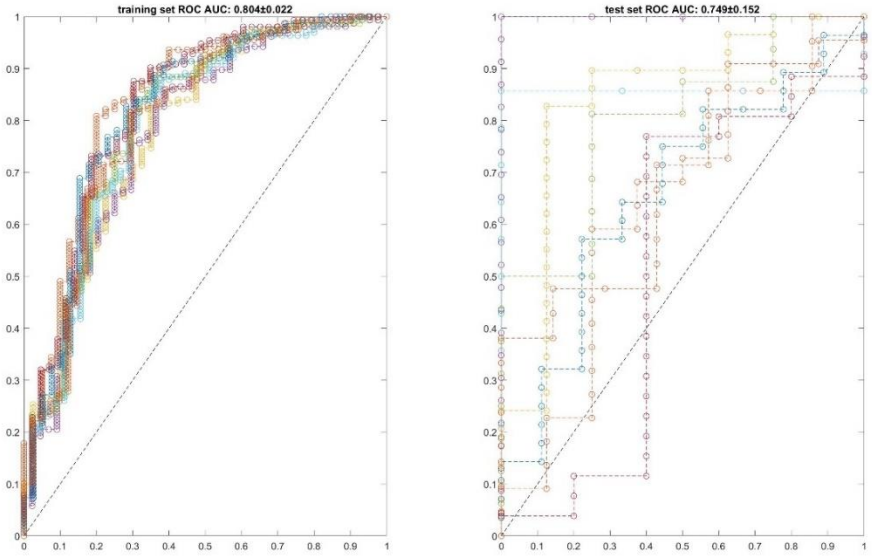

Figure 3.8 – ROC curve for subject 5

In Figure 3.9 is displayed the parameter AUC value with the aforementioned classification method. These results are generated during the classification of both the training-set and the test-set using the most discriminant features according to the Fisher's score. The blue bars represent the AUC parameter evaluated for the training-set of each subject, while the red bars represent the AUC parameter evaluated for the test-set of each subject; each bar is associated with a black vertical line that indicate the relative standard deviation. The 11^{th} group of bars displayed represent the average between subjects. The results obtained during the classification are consistent across all subjects: for the training-set the average AUC is 0.869±0.044, while for the test-set the average AUC is 0.777±0.051.

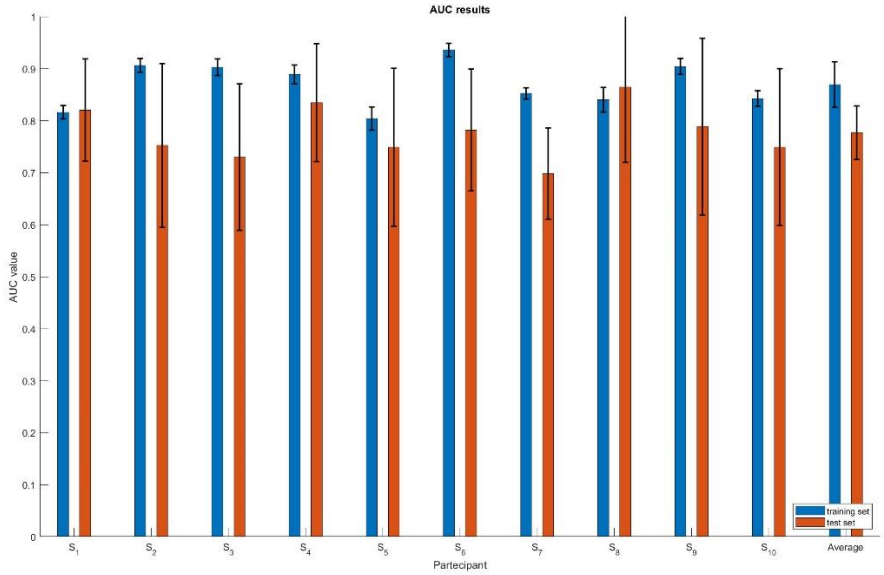

Figure 3.9 – AUC results

3.2.1 Delay application results

The results obtained after the application of the implementation delay are displayed in Figure 3.10. These data demonstrate the altered AUC distribution that occurs after the application of the implementation delay; this delay is equal to the time required to reach 20% of the maximum rotational velocity, which causes a shift in the acquisition's time window. The results are similar to the original one in fact, the average AUC for the training-set is 0.848±0.048 while the average AUC for the test-set is 0.765±0.098. Despite this high similarity with the original results, this different analysis highlights higher accuracy for the subject that showed a clear ErrP (e.g., subject 1) and lower accuracy for the remaining subjects (e.g., subject 5) that emerged during the Fz, Fcz and Cz analysis.

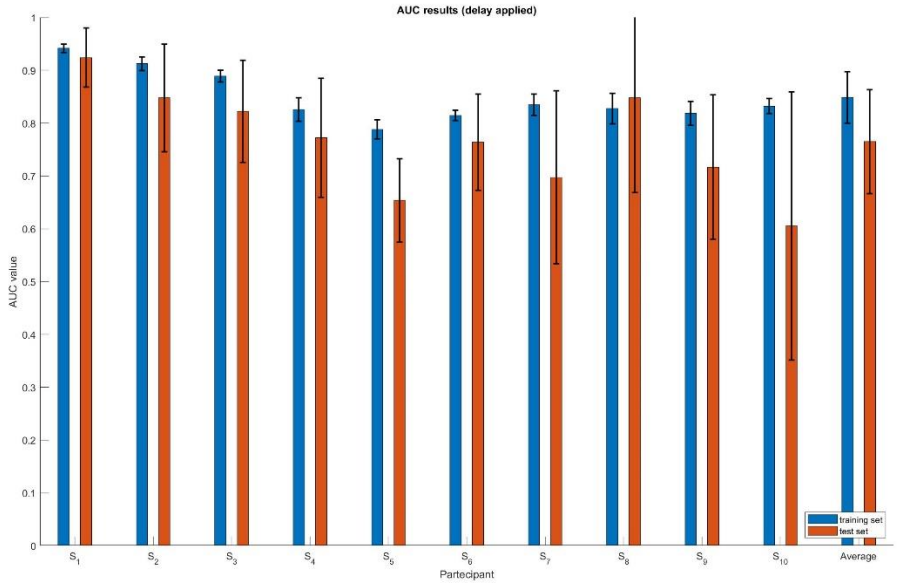

Figure 3.10 – AUC results with delay implementation

3.2.2 Different rotation results

In Figure 3.12 and Figure 3.13 are displayed the AUC distribution acquired following the division between different rotations. Employing the information acquired from the odometry for every command implemented we verified if the previous rotation of the wheelchair was performed in the same direction (which results in a concordant trial) or in the opposite direction (which results in a discordant trial). Analysing separately these two types of trials resulted in a much clearer ErrP detected which led to a significant improvement of the classification process (Figure 3.11 shows the grand average obtained after the division between the concordant rotation “CR” and the discordant rotation “DR”).

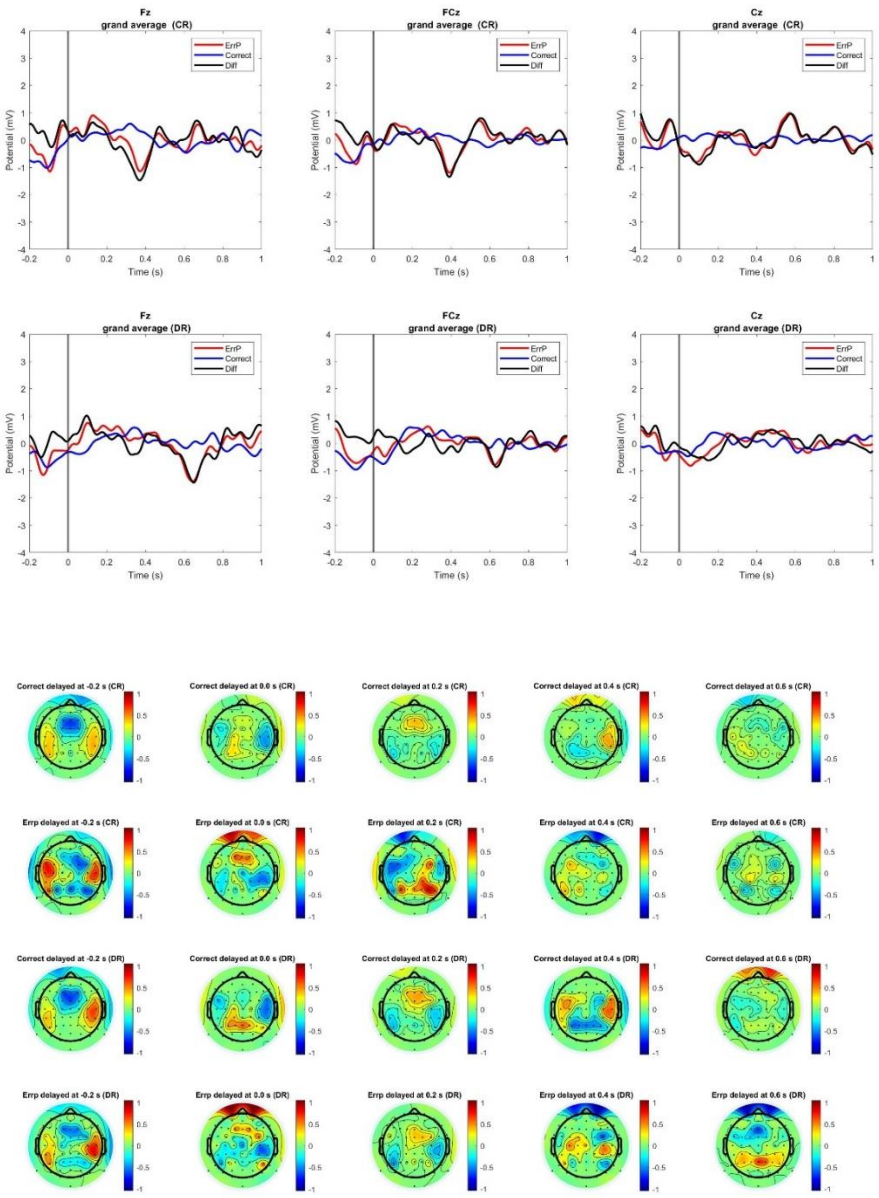

Figure 3.11 grand average obtained after the division between the concordant rotation "CR" and the discordant rotation "DR"

The classification improvement led to an increase of the AUC parameters for both the concordant rotation analysis (Figure 3.12) and the discordant rotation analysis (Figure 3.13); in fact, for the concordant rotation the average AUC value computed was 0.938±0.042 for the training-set and 0.803±0.102 for the test-set, while for the discordant rotation the average AUC value computed was 0.927±0.041 for the training-set and 0.800±0.091 for the test-set, which are both higher than the original value.

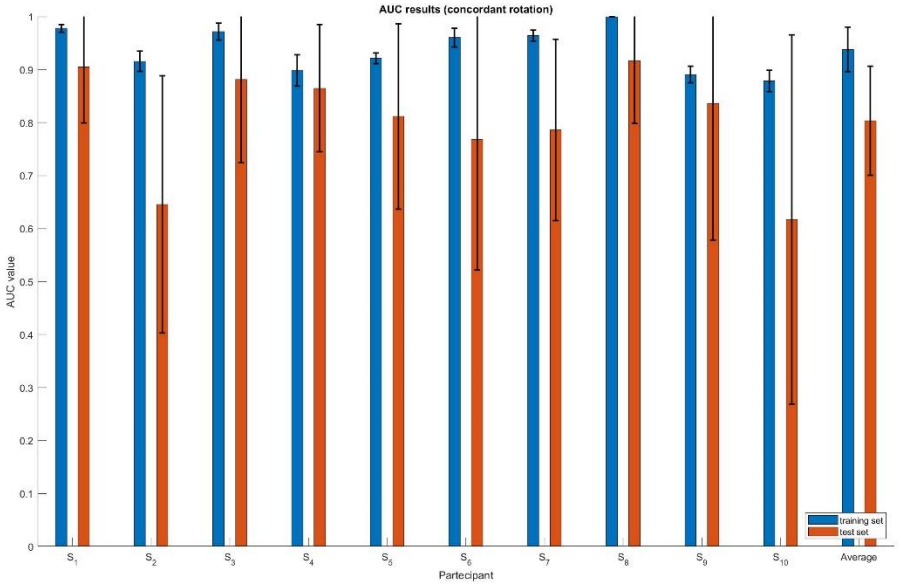

Figure 3.12 – AUC results for the concordant rotations

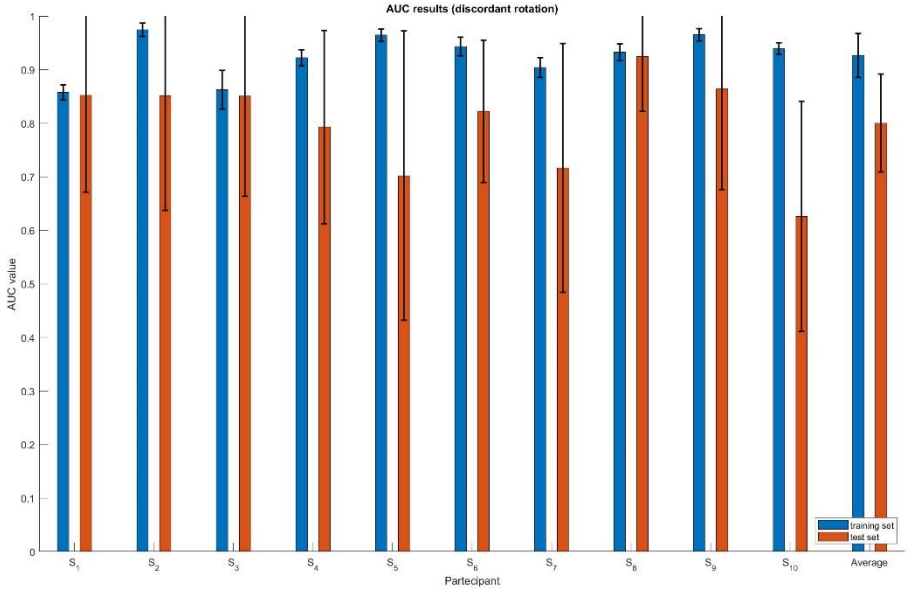

Figure 3.13 – AUC results for the discordant rotations

3.3.4 Results from the combination of the implementation delay and the division between different rotations

In Figure 3.14 and Figure 3.15 are displayed the results evaluated when both the additional analyses were performed simultaneously. These were the last result obtained and displayed the best AUC value for the concordant rotation while the AUC value for the discordant rotation were a bit lower compared to the previous results. In these final analyses the average AUC value for the concordant rotations was 0.942±0.046 for the training-set and 0.835±0.106 for the test-set while for the discordant rotations the average AUC value was 0.924±0.056 for the training-set and 0.783±0.098 for the test-set. Overall, the additional analyses show a significant improvement compared with the original AUC value obtained with the standard classification.

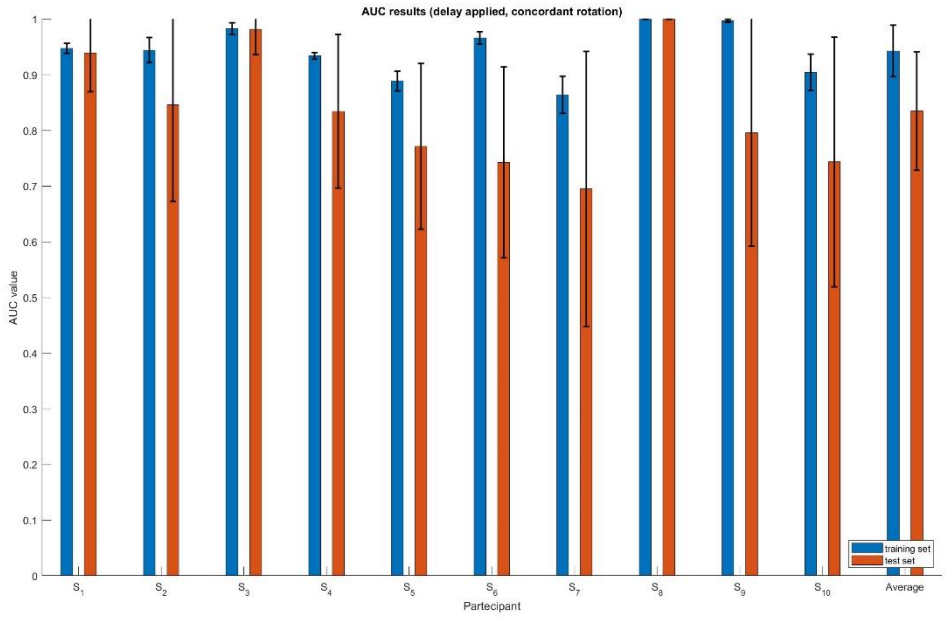

Figure 3.14 – AUC results for the concordant rotation with the delay implementation

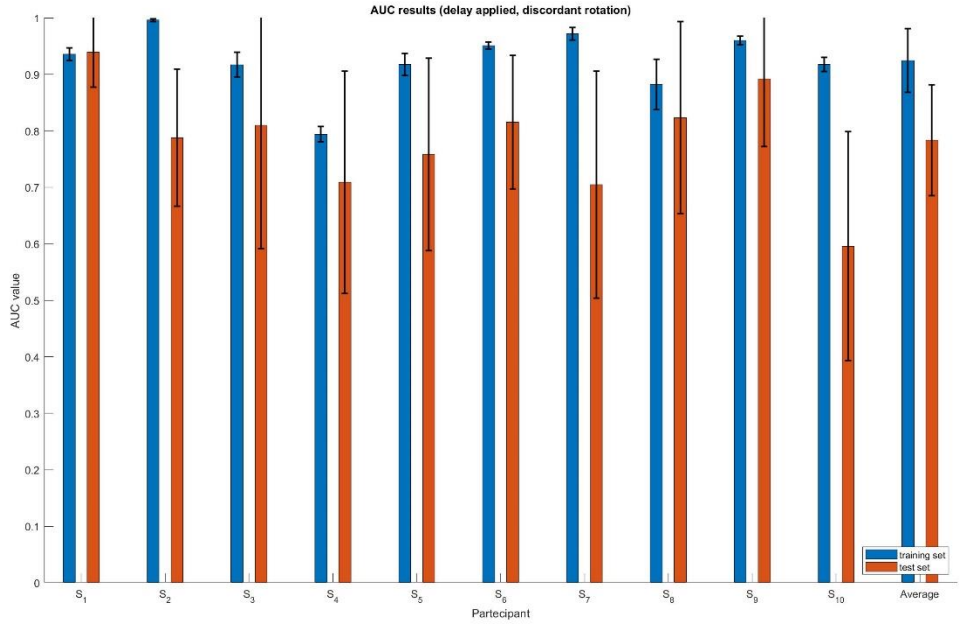

Figure 3.15 – AUC results for the discordant rotation with the delay implementation

4. Discussion

We have described and experimentally validated an approach for the detection and classification of the error-related potential during the navigation on a wheelchair.

Although the binary classification of the two types of trial produced good results, the classifier trained using the methods described was hampered by a number of issues that made it difficult to correctly classify the trials of each individual.

First of all, subjects who reported to have more experience using gamepads like the one used for the experiment displayed more stable and controlled values of amplitudes during the measurements.

This means that the training period given to subject wasn't enough long to get familiar with the control system, which led to anomalies during the measurement of the more inexperienced subjects; in fact, these participants occasionally misread the placement of the buttons that needed to be pressed in order to rotate the wheelchair and confused the buttons to press to execute the desired command, due to the lack of experience with the gamepad; because of this, error potentials have been generated even when a correct trial has been acquired even though these potentials were unrelated to the outcome of the rotation, which has unavoidably increased the difficulty of classifying training-set and test-set data.

The final aspect worth mentioning is relative to an additional reason of difficulty for the user generated during the measurement due to the technical characteristics of the wheelchair; in fact, only the two front wheels of the wheelchair are motorized wheels while the two back-wheels follow the overall movement of the chair according to the direction imposed from the motorized wheels, this means that every command delivered to the wheelchair modify the orientation of the front wheels while the back wheels need to adjust their orientation independently.

Due to this technical characteristic of the wheelchair, after the complete implementation of a rotational command the device tries to resume its linear trajectory by setting the rotational speed of the front wheels 0 km/h, while the two back wheels remain oriented in the direction of previous rotation; consequently, after the completion of the command delivered, the wheelchair continued to rotate for a few milliseconds according to the direction imposed form the previous command.

Even if this fault was correctable, we decided at the begging of the measurement period to leave this aspect unchanged, because it would have forced the user to

execute more rotational command in order to follow the correct path, which results in more opportunities to generate a command inversion and new ErrPs.

Due to the interaction of these parameters and the inherent variation among the different brain responses, a dataset with a wide range of responses in terms of detected amplitudes and latencies has been produced.

The classifier trained according to the methods described previously showed good results in the process of binary division of the two types of trial despite the multiple factors aforementioned; additional considerations were made after the analysis of the EEG signals in order to significantly increase the value of the accuracy of the measurement process.

The first additional analysis parameter that was considered was the delay generated during the implementation of a command. During the process of acquiring EEG signals, a time window of two seconds was examined starting from the precise moment the command was delivered to the wheelchair; this analysis considers that the brain detects the change of speed in a certain direction as soon as the command is received form the wheelchair. This assumption is not correct because in order to represent this scenario the wheelchair should instantly reach the required speed during the command implementation and therefore have an infinite acceleration. To evaluate how the chair was accelerating gradually, the data derived from odometry, relative to the rotational velocity section, were evaluated.

During the entire acquisition process, the wheelchair reached the desired maximum speed with variable acceleration between different trials; this irregularity is connected to the technical characteristics of the back wheels of the wheelchair discussed previously.

Requesting rotations in opposite directions imposes to the motorized wheels a drastic change of direction, which is why the secondary wheels need a few milliseconds to be able to orient in the correct direction and then perform the desired acceleration. Since each command is run under different conditions, it is impossible to evaluate a constant acceleration because every time a trial is completed the back wheels are positioned in a different way.

To solve this issue, a percentage threshold was used to analyse the rotational speed of the device. The algorithm employed recognized the maximum value of rotational speed detected for each command and computed an acceptable threshold at the point when the speed reached 20% of the maximum speed desired.

Additionally, even though the nominal speed sent to the device was constant, the practical value recorded was never constant based to any field imperfection of the laboratory and the placement of the secondary wheels, which either accompanied or opposed the rotation (depending on the kind of commands received previously); this is another reason why it was necessary to generate an adaptive threshold and not a static one. The point highlighted by this process was therefore considered as an initial point of acquisition, which corresponds to the moment in which the brain was able to correctly perceive what kind of rotation was taking place.

This step led to a dynamic translation of the capture window for each trial and an overall time alignment of the peaks recorded in the various trials and allowed to increase the recorded accuracy.

The second additional analysis was to consider in a separate way the trials that are connected to a concordant or discordant rotation compared with the previous command delivered.

This analysis was made in order to consider the type of response of the wheelchair according to the orientation of the back wheels at the end of the previous command. If during the measurement the subject required to execute two commands in opposite directions, the wheelchair had to perform a settling process for a few milliseconds before it could perform the correct rotation.

This consideration, besides being important for the calculation of the delay, highlights the importance of the subdivision between concordant rotations and discordant rotations: if the intended rotational control is carried out in the same rotational direction as the previous one, the non-driving wheels are already be correctly oriented; on the contrary, when the required control is relative to an inverse rotational direction to the previous one, the wheels must perform the alignment movement before rotating correctly, this generates different latencies for every points of interest and therefore complicates the classification process; We evaluated that dividing these types of trial could significantly increase overall accuracy due to the time difference between the averages of the two types of trial.

The results show that, by performing a differentiated classification only on concordant and discordant type trials leads to a considerable increase in the AUC parameter, especially considering to the concordant rotations; the reason why the classification for the discordant rotations have overall lower accuracy across

subjects is similar to the motivation explained previously for the selection of a dynamic threshold.

In fact, the discordant rotation generates a process of wheel alignment before the command implementation, this process is not constant and varies depending on how much time has passed after the completion of the previous rotation; after completing a rotational command the wheelchair needs a few milliseconds to realign the back wheels in order to continue its linear trajectory; this leads the wheelchair to rotate differently according to the current position of the wheels. The EEG signals evaluated in these conditions have different latencies of the important peaks of the ErrP.

For this reason, the averages of the signals recorded in the discordant rotations are less marked than the concordant rotations and therefore more difficult to classify. Nevertheless, analysing these types of trial separately from the concordant ones leads to a considerable improvement of the classification process with a relative increase of accuracy found by the AUC parameter.

Overall, these two analyses were key in the process of perfecting the classification algorithm and allowed to obtain excellent results for all registered subjects.

5. Conclusions

Two key points in the research have been confirmed by the results of these experiments. First, it was possible to confirm the actual existence of a distinct physiological signal that could be traced to the waveform of the error-potential in a measurement environment and under previously untested conditions. Secondly it has been confirmed that the waveform of the ErrP detected is consistent throughout the whole analysis, thus confirming the possibility of a classification method for the ErrP thus detected.

In order to significantly improve the research process to assist people with paraplegia and quadriplegia it is crucial to emphasize the ability to detect such a signal in dynamic scenarios, where the user is forced to make decisions to travel in a constrained location.

Up until this point, measures were carried out in environments that did not require the patient to pay attention to both the immediate surroundings and the task that needed to be performed; the good results obtained from the classification process described support the idea of creating and incorporating a system of self-correction of the wheelchair's trajectory in the event that a command not intended by the user is carried out.

From the results of this study, it is possible to obtain useful information to continue future experiments concerning wheelchair error potentials.

In order to ensure outcomes of a higher level than those obtained in this study, a systematic process of refinement of the acquisition and classification system is required in order to perfect this job; first, the statistical sample must be expanded to include more than the ten subjects that are insufficient to establish an absolute validity requirement, in order to acquire and analyse more unique brain responses, along with the relative unique ErrP waveform.

Secondly, it is necessary to evaluate the capacity of the brain to generate a clear EEG signal under less controlled circumstances, attempting to mimic a real environment with noises and uneven surfaces to comprehend the different behaviour of people when they face multiple stimulus at once; a way to implement this aspect would be to remove the simple cross to fixate during the measurement, in order to comprehend how much the eye movement inherit the clear ErrP classification; alternatively, the subject could navigate towards a goal without a

predefined path to follow in order to understand how different decisions related to the completion of a non-predefined course could vary the brain response.

For the last aspect that needs to be improved, it is important to test different features form the one tested during this experiment, while also testing other classification algorithm in order to ensure an extremely high ability to recognize the type of brain response.

Despite the limitations and weaknesses in this type of testing, it can nevertheless be concluded that, considering the good ability to interpret the system even in non-standard conditions, this study has proven to be valid to set a statistically significant baseline for the classification of error-related potential during wheelchair navigation.

6. Appendix section

6.1 Appendix 1: Fz, Fcz and Cz

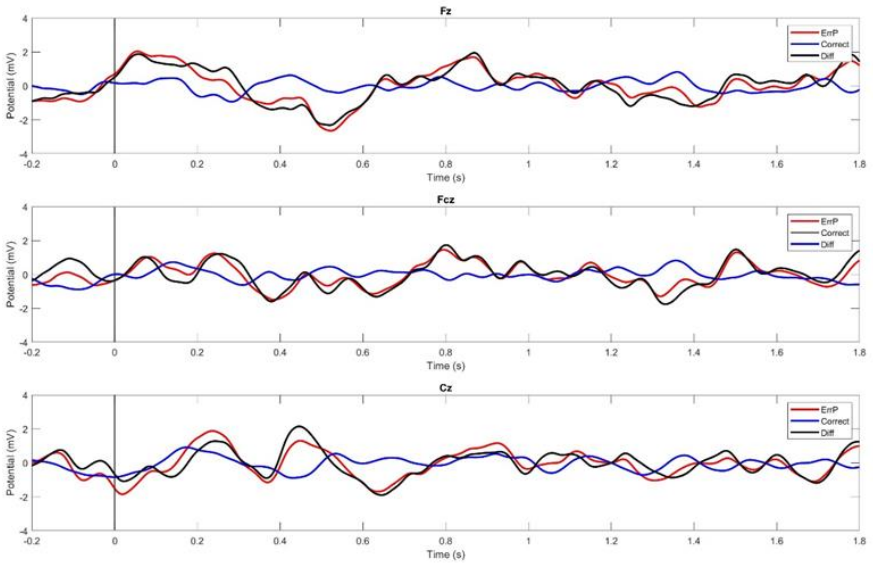

Fz, Fcz and Cz of Subject 1

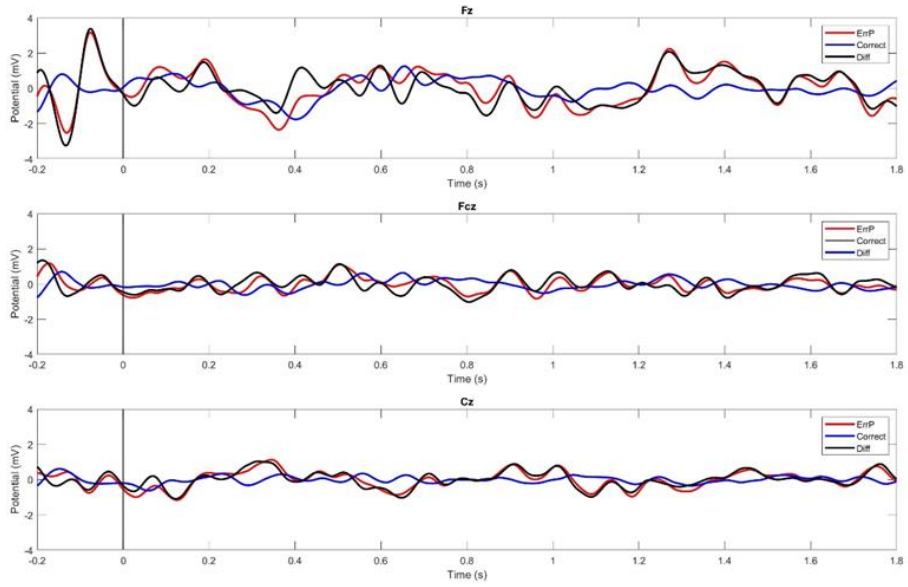

Fz, Fcz and Cz of Subject 2

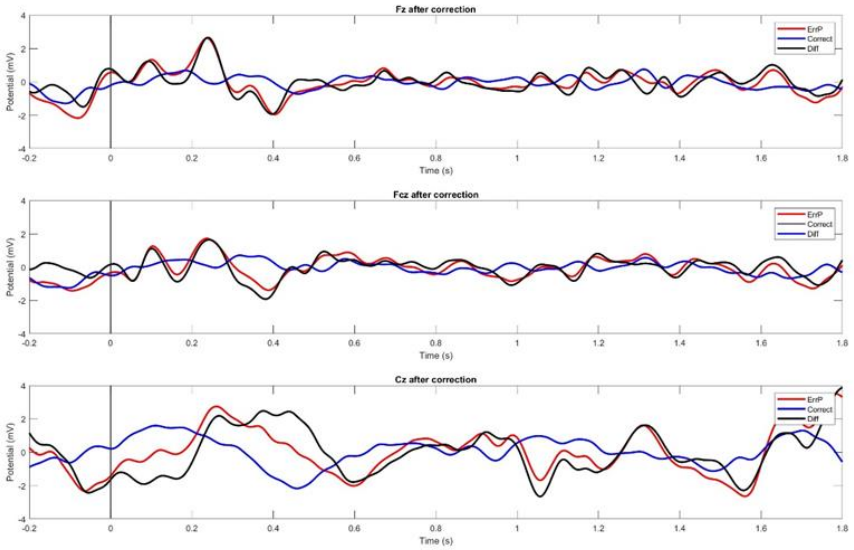

Fz, Fcz and Cz of Subject 3

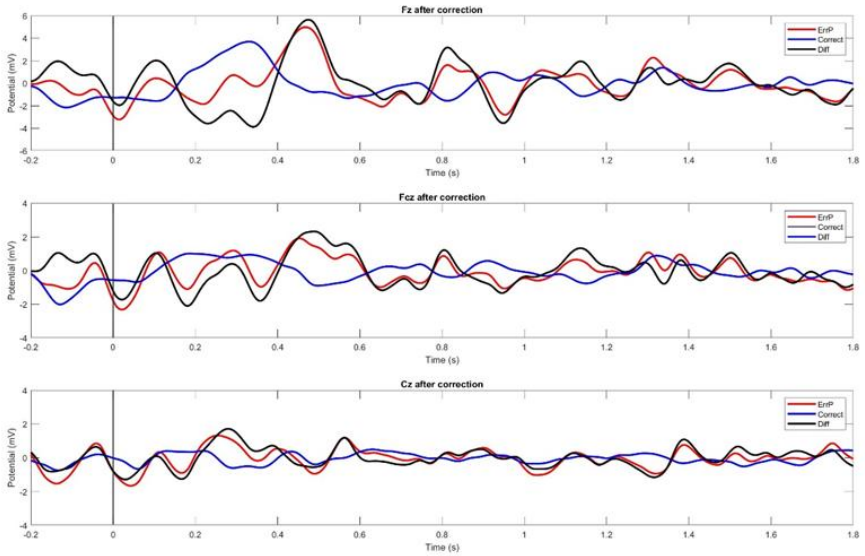

Fz, Fcz and Cz of Subject 4

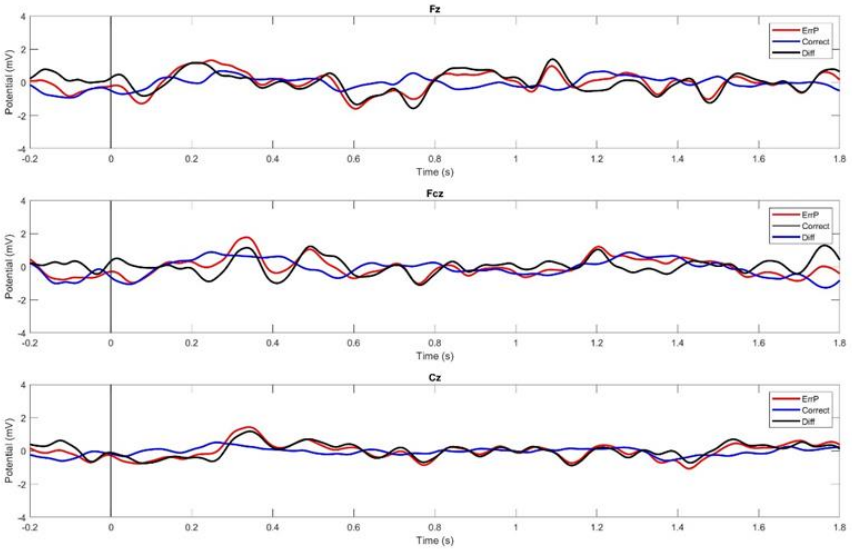

Fz, Fcz and Cz of Subject 5

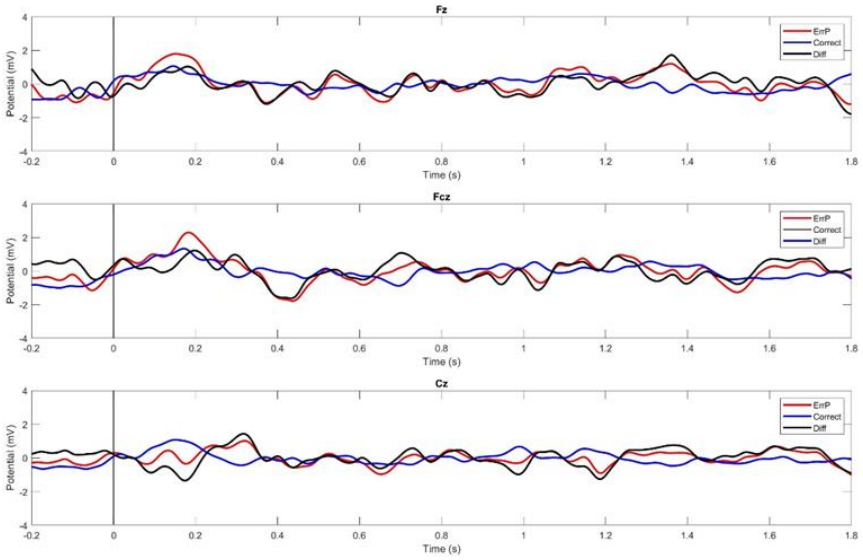

Fz, Fcz and Cz of Subject 6

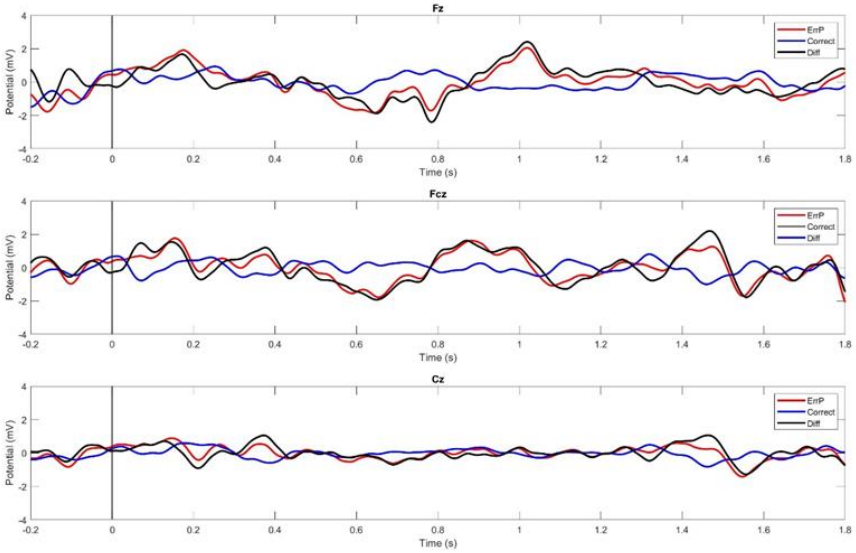

Fz, Fcz and Cz of Subject 7

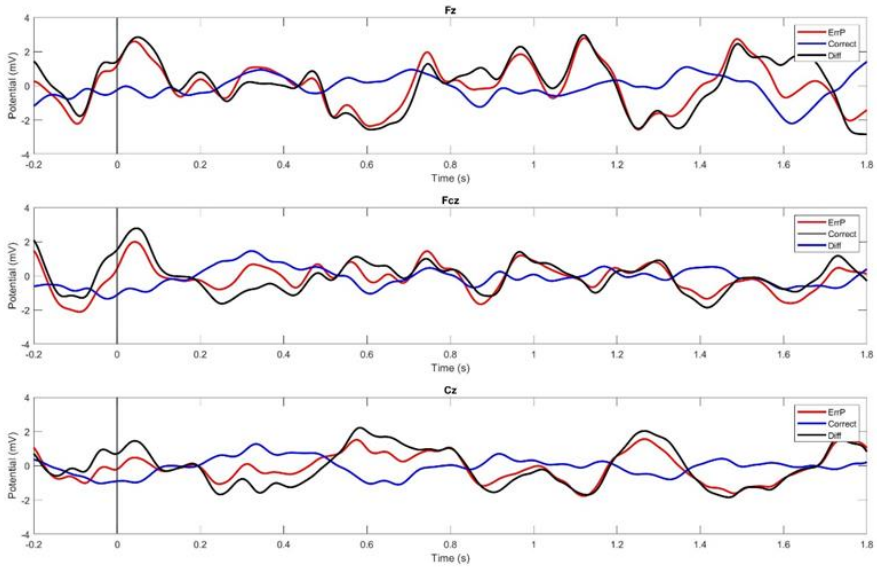

Fz, Fcz and Cz of Subject 8

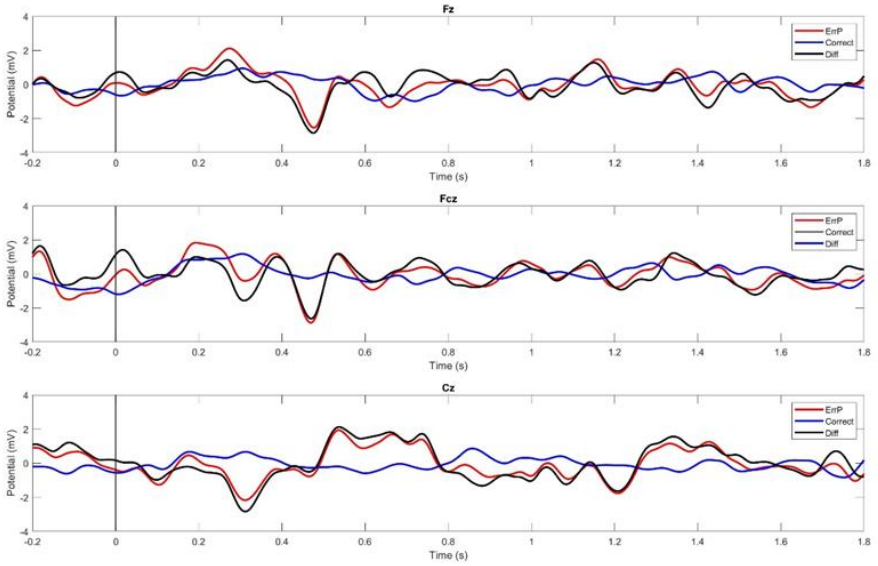

Fz, Fcz and Cz of Subject 9

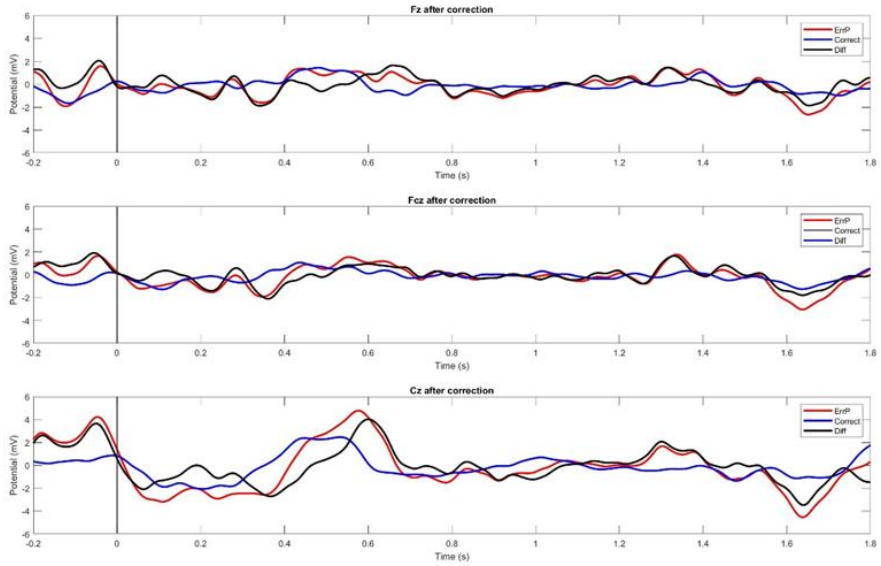

Fz, Fcz and Cz of Subject 10

6.2 Appendix 2: Topographic view

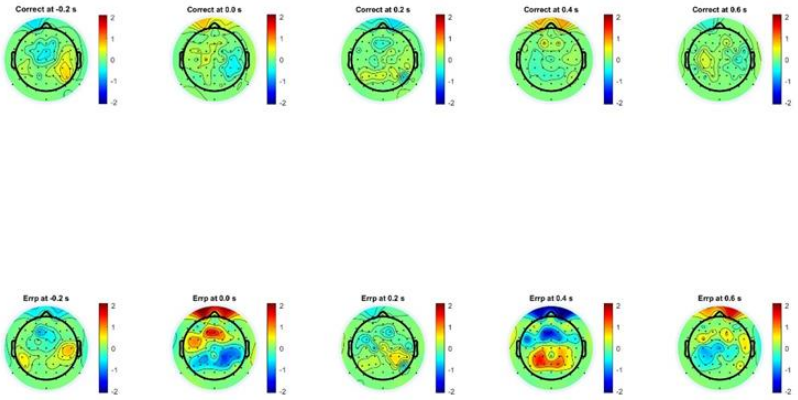

Topographic view of subject 1

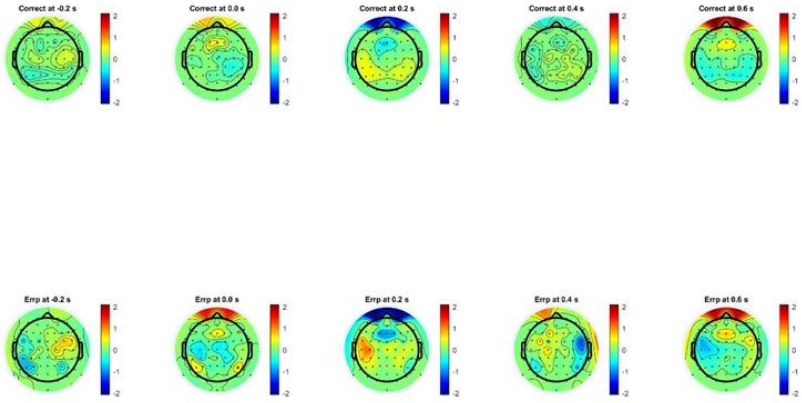

Topographic view of subject 2

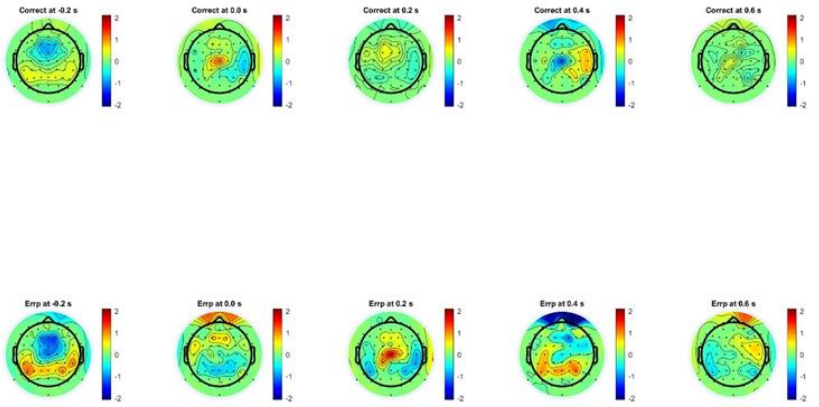

Topographic view of subject 3

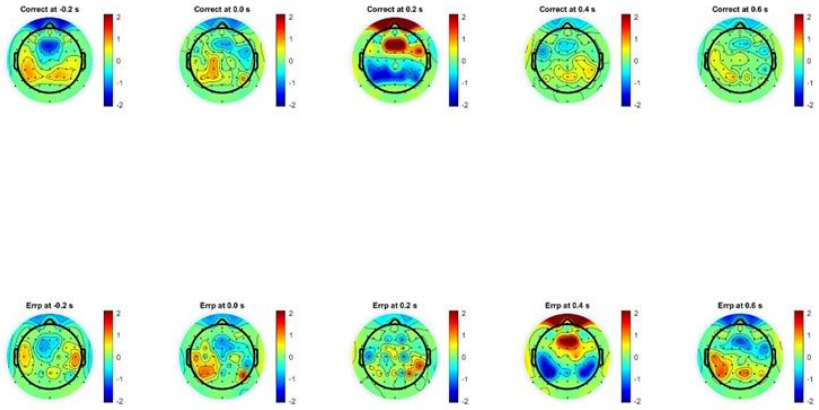

Topographic view of subject 4

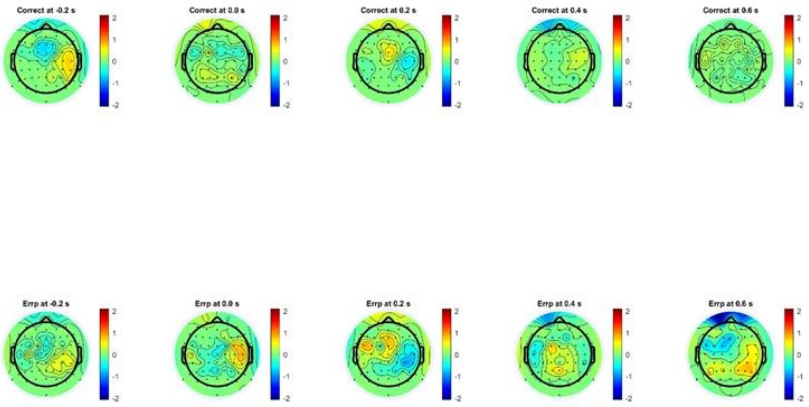

Topographic view of subject 5

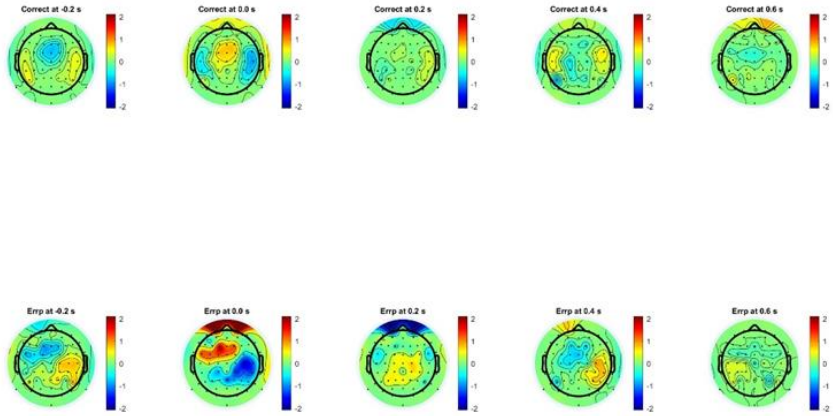

Topographic view of subject 6

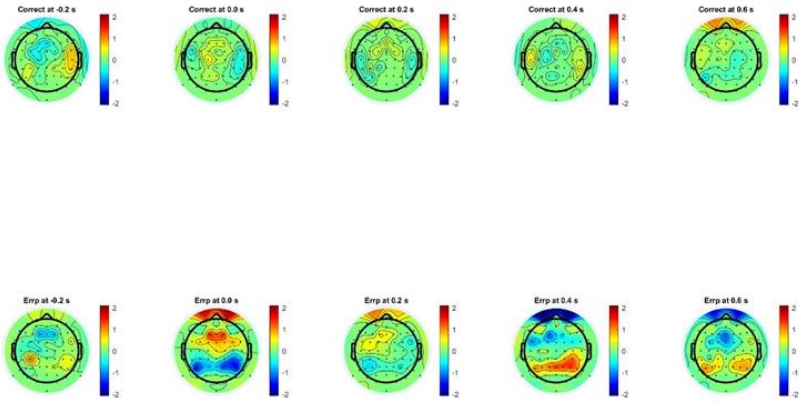

Topographic view of subject 7

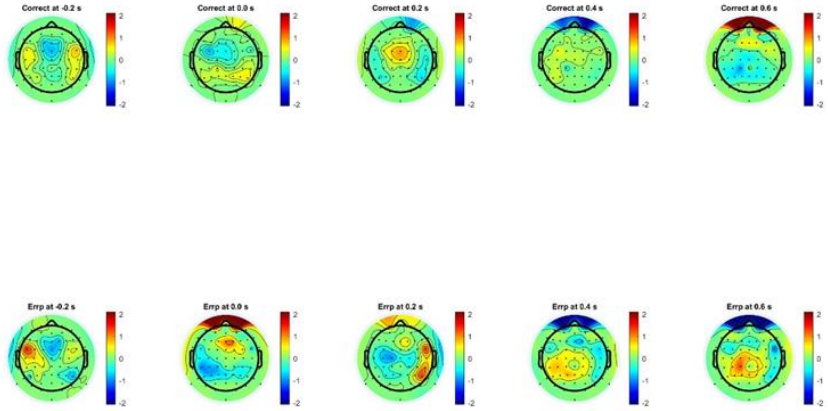

Topographic view of subject 8

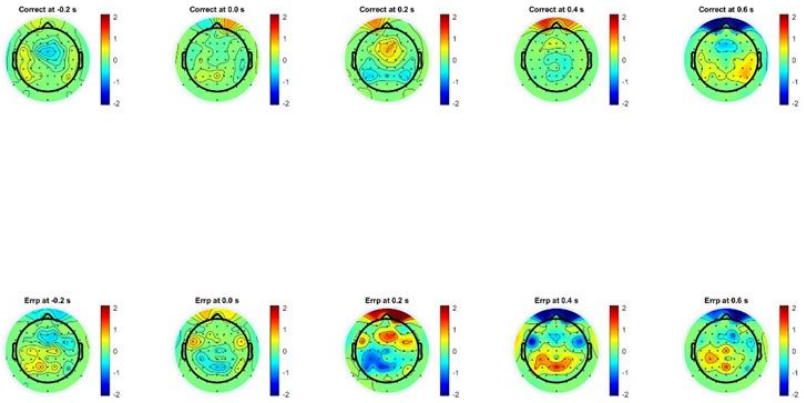

Topographic view of subject 9

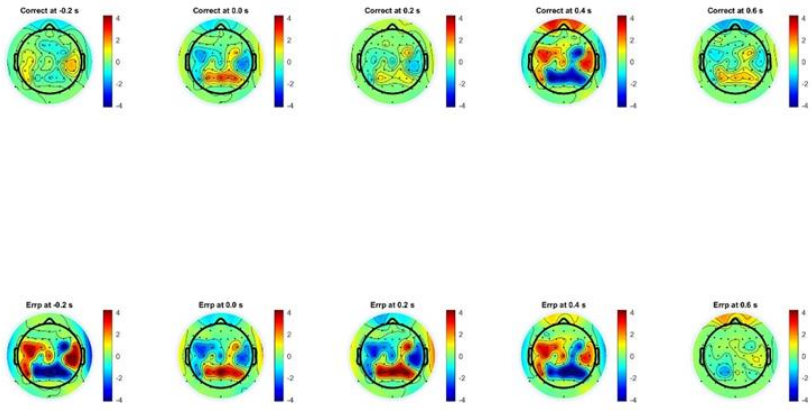

Topographic view of subject 10

6.3 Appendix 3: ROC curves

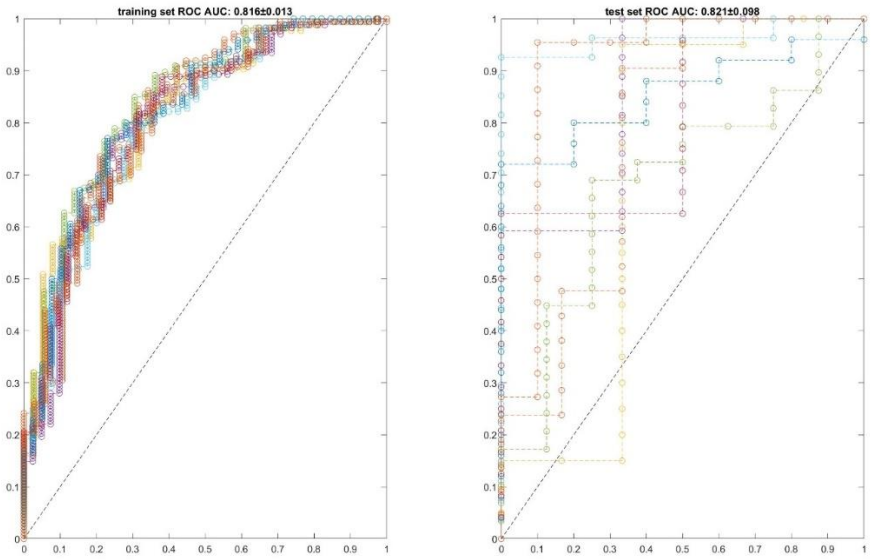

ROC curve for subject 1

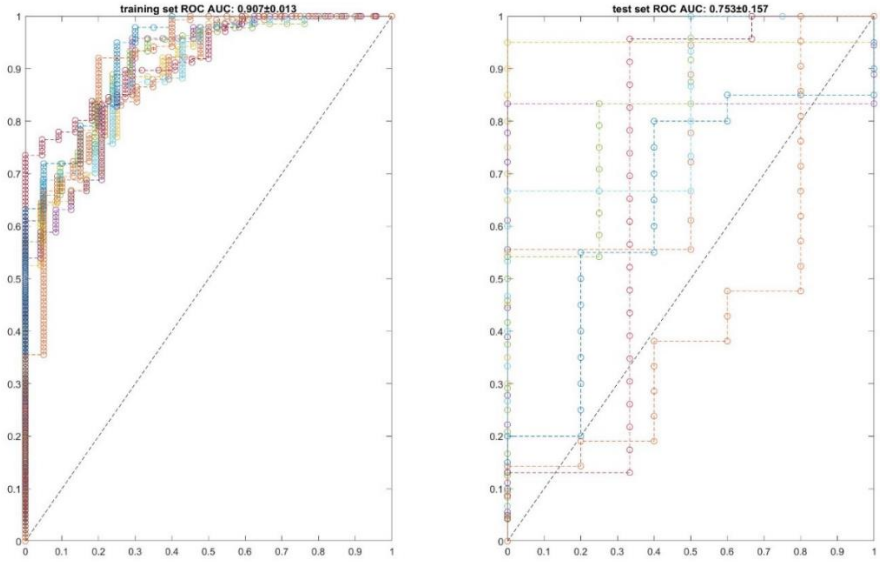

ROC curve for subject 2

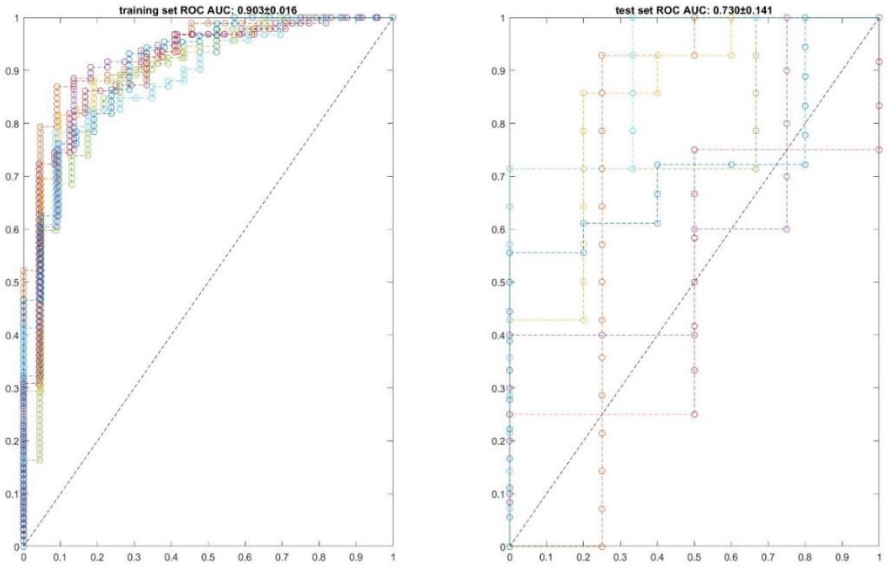

ROC curve for subject 3

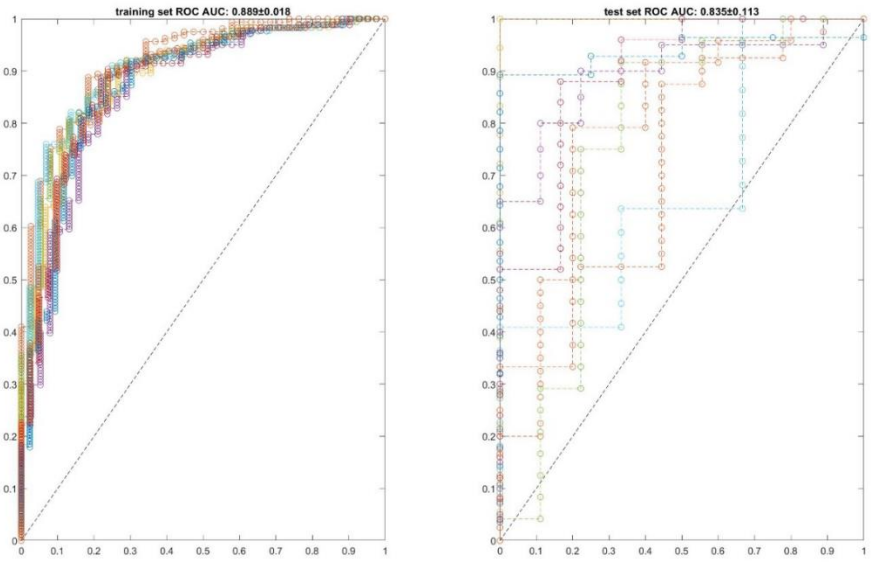

ROC curve for subject 4

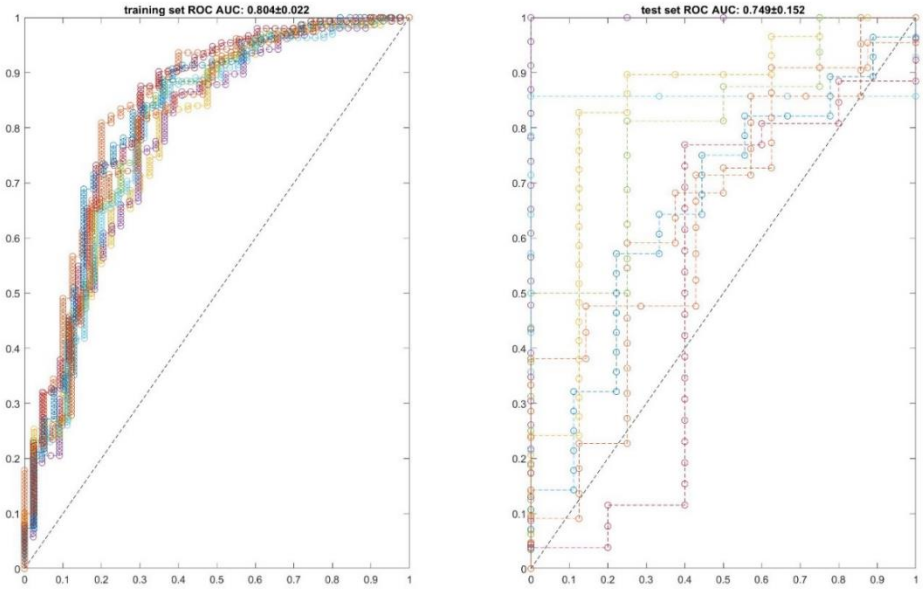

ROC curve for subject 5

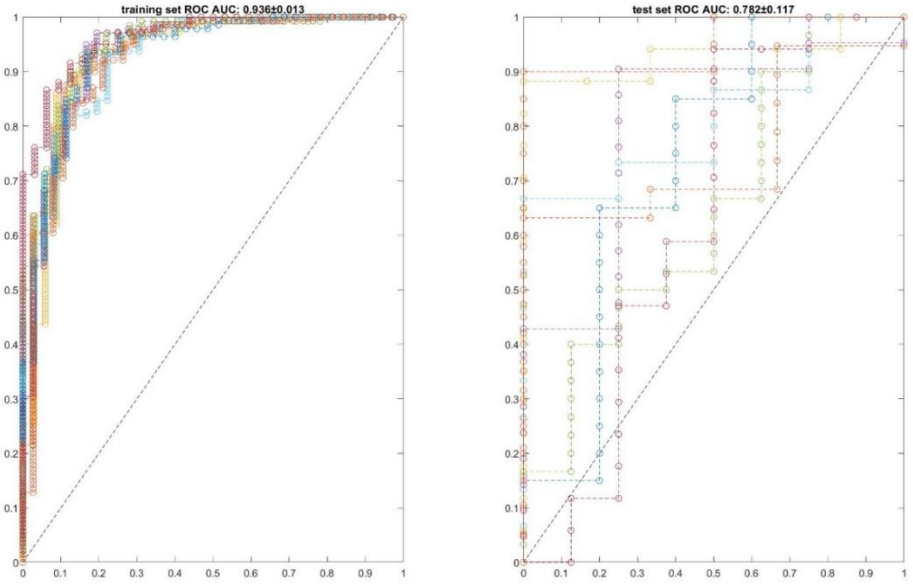

ROC curve for subject 6

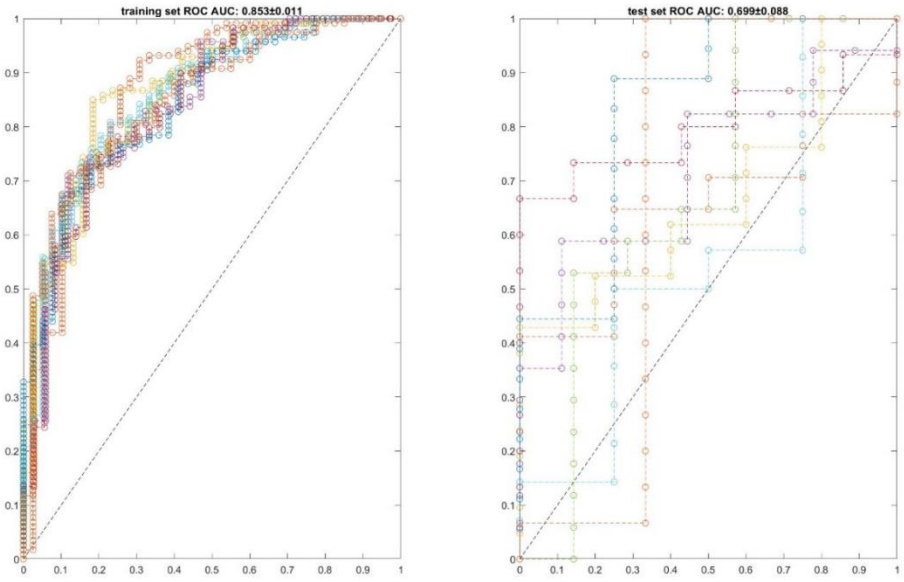

ROC curve for subject 7

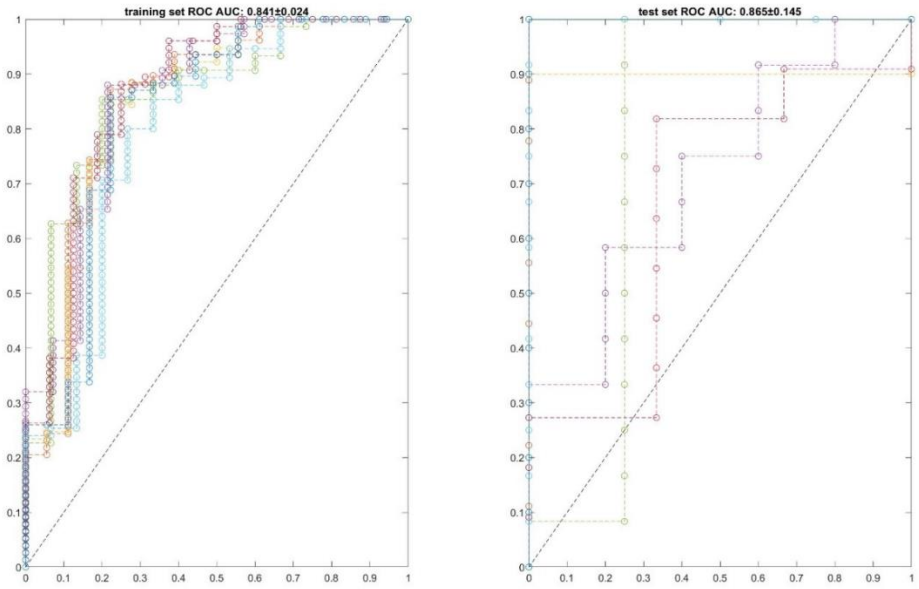

ROC curve for subject 8

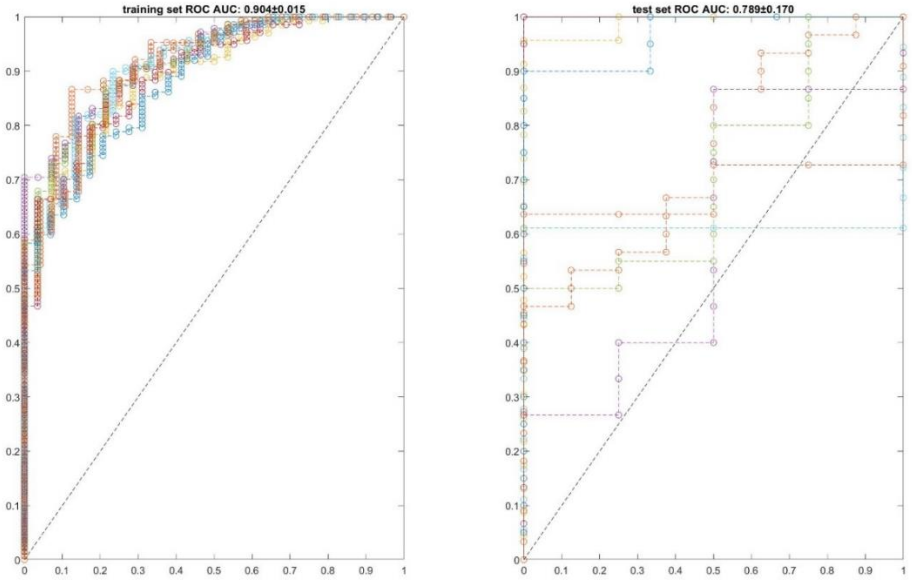

ROC curve for subject 9

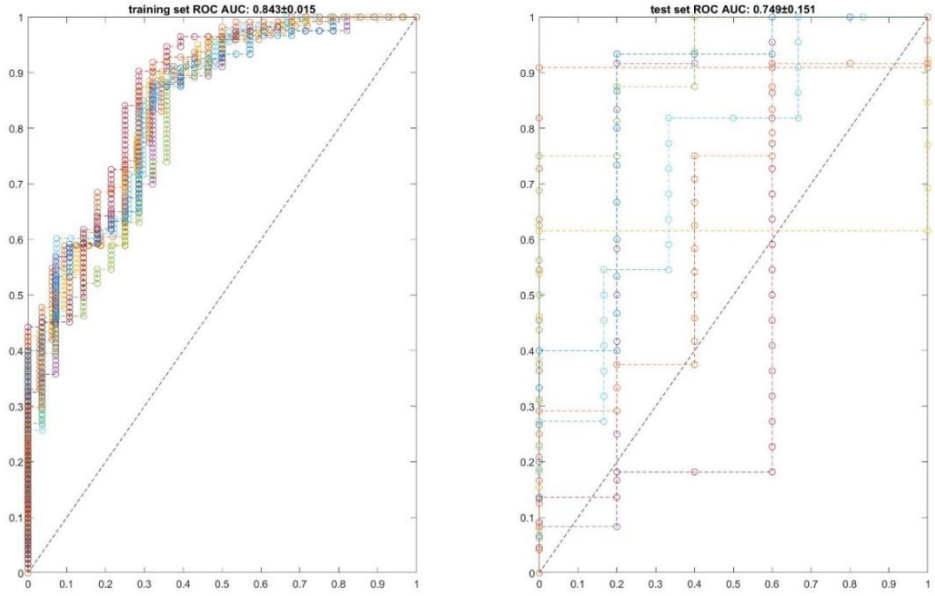

ROC curve for subject 10

7. Bibliography

Abiri, R., Borhani, S., Sellers, E. W., Jiang, Y., & Zhao, X. (2019). A comprehensive review of EEG-based brain–computer interface paradigms. *Journal of Neural Engineering*, *16*(1), 011001. https://doi.org/10.1088/1741-2552/aaf12e

Alhaddad, M. (2022). *Common Average Reference (CAR) Improves P300 Speller*.

Amiri, S., Fazel-Rezai, R., & Asadpour, V. (2013). A review of hybrid brain-computer interface systems. *Advances in Human-Computer Interaction*, *2013*, 1:1. https://doi.org/10.1155/2013/187024

Bakardjian, H., Tanaka, T., & Cichocki, A. (2011). Emotional faces boost up steady-state visual responses for brain-computer interface. *Neuroreport*, *22*(3), 121–125. https://doi.org/10.1097/WNR.0b013e32834308b0

Bashashati, A., Ward, R. K., & Birch, G. E. (2007). Towards development of a 3-state self-paced brain-computer interface. *Computational Intelligence and Neuroscience*, 84386. https://doi.org/10.1155/2007/84386

Bera, T. K. (2015). Noninvasive Electromagnetic Methods for Brain Monitoring: A Technical Review. In A. E. Hassanien & A. T. Azar (Eds.), *Brain-Computer Interfaces: Current Trends and Applications* (pp. 51–95). Springer International Publishing. https://doi.org/10.1007/978-3-319-10978-7_3

Bhattacharyya, S., Konar, A., & Tibarewala, D. N. (2014). Motor imagery, P300 and error-related EEG-based robot arm movement control for rehabilitation purpose. *Medical & Biological Engineering & Computing*, *52*(12), 1007–1017. https://doi.org/10.1007/s11517-014-1204-4

Bhattacharyya, S., Konar, A., & Tibarewala, D. N. (2017). Motor imagery and error related potential induced position control of a robotic arm. *IEEE/CAA Journal of Automatica Sinica*, *4*(4), 639–650. https://doi.org/10.1109/JAS.2017.7510616

Bin, G., Gao, X., Wang, Y., Hong, B., & Gao, S. (2009). VEP-based brain-computer interfaces: Time, frequency, and code modulations [Research Frontier]. *IEEE Computational Intelligence Magazine*, *4*(4), 22–26. https://doi.org/10.1109/MCI.2009.934562

Birbaumer, N. (2006). Breaking the silence: Brain–computer interfaces (BCI) for communication and motor control. *Psychophysiology*, *43*(6), 517–532. https://doi.org/10.1111/j.1469-8986.2006.00456.x

Borhani, S., Abiri, R., Zhao, X., & Jiang, Y. (2017, November). A Transfer Learning Approach towards Zero-training BCI for EEG-Based Two Dimensional Cursor Control. *Society for Neuroscience 2017 Meeting (SfN2017)*. https://hal.archives-ouvertes.fr/hal-01640834

Cawley, G. C., & Talbot, N. L. C. (2003). Efficient leave-one-out cross-validation of kernel fisher discriminant classifiers. *Pattern Recognition*, *36*(11), 2585–2592. https://doi.org/10.1016/S0031-3203(03)00136-5

Chavarriaga, R., & Millan, J. del R. (2010). Learning From EEG Error-Related Potentials in Noninvasive Brain-Computer Interfaces. *IEEE Transactions on Neural Systems and Rehabilitation Engineering*, *18*(4), 381–388. https://doi.org/10.1109/TNSRE.2010.2053387

Chi, Y. M., Wang, Y.-T., Wang, Y., Maier, C., Jung, T.-P., & Cauwenberghs, G. (2012). Dry and Noncontact EEG Sensors for Mobile Brain–Computer Interfaces. *IEEE Transactions on Neural Systems and Rehabilitation Engineering*, *20*(2), 228–235. https://doi.org/10.1109/TNSRE.2011.2174652

Dal Seno, B., Matteucci, M., & Mainardi, L. (2010a). Online detection of P300 and error potentials in a BCI speller. *Computational Intelligence and Neuroscience*, 307254. https://doi.org/10.1155/2010/307254

Dal Seno, B., Matteucci, M., & Mainardi, L. T. (2010b). The Utility Metric: A Novel Method to Assess the Overall Performance of Discrete Brain–Computer Interfaces. *IEEE Transactions on Neural Systems and Rehabilitation Engineering*, *18*(1), 20–28. https://doi.org/10.1109/TNSRE.2009.2032642

Diez, P. F., Mut, V. A., Avila Perona, E. M., & Laciar Leber, E. (2011). Asynchronous BCI control using high-frequency SSVEP. *Journal of NeuroEngineering and Rehabilitation*, *8*, 39. https://doi.org/10.1186/1743-0003-8-39

Dobrea, M.-C., & Dobrea, D. M. (2009). The selection of proper discriminative cognitive tasks—A necessary prerequisite in high-quality BCI applications. *2009 2nd International Symposium on Applied Sciences in Biomedical and Communication Technologies*, 1–6. https://doi.org/10.1109/ISABEL.2009.5373706

Dong, S.-Y., Kim, B.-K., & Lee, S.-Y. (2016). EEG-Based Classification of Implicit Intention During Self-Relevant Sentence Reading. *IEEE Transactions on Cybernetics*, *46*(11), 2535–2542. https://doi.org/10.1109/TCYB.2015.2479240

Donoghue, J. P. (2002). Connecting cortex to machines: Recent advances in brain interfaces. *Nature Neuroscience*, *5*(11), Article 11. https://doi.org/10.1038/nn947

Ehrlich, S. K., & Cheng, G. (2018). Human-agent co-adaptation using error-related potentials. *Journal of Neural Engineering*, *15*(6), 066014. https://doi.org/10.1088/1741-2552/aae069

Fan, J., Upadhye, S., & Worster, A. (2006). Understanding receiver operating characteristic (ROC) curves. *CJEM*, *8*(01), 19–20. https://doi.org/10.1017/S1481803500013336

Fernández-Rodríguez, Á., Velasco-Álvarez, F., & Ron-Angevin, R. (2016). Review of real brain-controlled wheelchairs. *Journal of Neural Engineering*, *13*(6), 061001. https://doi.org/10.1088/1741-2560/13/6/061001

Ferrez, P. W., & del R Millan, J. (2008). Error-related EEG potentials generated during simulated brain-computer interaction. *IEEE Transactions on Bio-Medical Engineering*, *55*(3), 923–929. https://doi.org/10.1109/TBME.2007.908083

Golub, M. D., Chase, S. M., Batista, A. P., & Yu, B. M. (2016). Brain-computer interfaces for dissecting cognitive processes underlying sensorimotor control. *Current Opinion in Neurobiology*, *37*, 53–58. https://doi.org/10.1016/j.conb.2015.12.005

Grozea, C., Voinescu, C. D., & Fazli, S. (2011). Bristle-sensors—Low-cost flexible passive dry EEG electrodes for neurofeedback and BCI applications. *Journal of Neural Engineering*, *8*(2), 025008. https://doi.org/10.1088/1741-2560/8/2/025008

Holz, E. M., Botrel, L., Kaufmann, T., & Kübler, A. (2015). Long-term independent brain-computer interface home use improves quality of life of a patient in the locked-in state: A case study. *Archives of Physical Medicine and Rehabilitation*, *96*(3 Suppl), S16-26. https://doi.org/10.1016/j.apmr.2014.03.035

Iturrate, I., Montesano, L., & Chavarriaga, R. (2011). *Spatio-Temporal Filtering for EEG Error Related Potentials*. 4.

Iturrate, I., Montesano, L., & Minguez, J. (2010a). Single trial recognition of error-related potentials during observation of robot operation. *Annual International Conference of the IEEE Engineering in Medicine and Biology*

Society. IEEE Engineering in Medicine and Biology Society. Annual International Conference, *2010*, 4181–4184. https://doi.org/10.1109/IEMBS.2010.5627380

Iturrate, I., Montesano, L., & Minguez, J. (2010b). Robot reinforcement learning using EEG-based reward signals. *2010 IEEE International Conference on Robotics and Automation*, 4822–4829. https://doi.org/10.1109/ROBOT.2010.5509734

Iturrate, I., Omedes, J., & Montesano, L. (2013). Shared control of a robot using EEG-based feedback signals. *Proceedings of the 2nd Workshop on Machine Learning for Interactive Systems: Bridging the Gap Between Perception, Action and Communication*, 45–50. https://doi.org/10.1145/2493525.2493533

joy—ROS Wiki. (2022). http://wiki.ros.org/joy

Jrad, N., & Congedo, M. (2012). Identification of spatial and temporal features of EEG. *Neurocomputing*, *90*, 66–71. https://doi.org/10.1016/j.neucom.2012.02.032

Kim, J. H., Kim, B. C., Byun, Y. T., Jhon, Y. M., Lee, S., Woo, D. H., & Kim, S. H. (2004). All-Optical AND Gate Using Cross-Gain Modulation in Semiconductor Optical Amplifiers. *Japanese Journal of Applied Physics*, *43*(2R), 608. https://doi.org/10.1143/JJAP.43.608

Kumar, A., Gao, L., Pirogova, E., & Fang, Q. (2019). A Review of Error-Related Potential-Based Brain–Computer Interfaces for Motor Impaired People. *IEEE Access*, *7*, 142451–142466. https://doi.org/10.1109/ACCESS.2019.2944067

Längkvist, M., Karlsson, L., & Loutfi, A. (2014). A review of unsupervised feature learning and deep learning for time-series modeling. *Pattern Recognition Letters*, *42*, 11–24. https://doi.org/10.1016/j.patrec.2014.01.008

Lee, P.-L., Yeh, C.-L., Cheng, J. Y.-S., Yang, C.-Y., & Lan, G.-Y. (2011). An SSVEP-based BCI using high duty-cycle visual flicker. *IEEE Transactions on Bio-Medical Engineering*, *58*(12), 3350–3359. https://doi.org/10.1109/TBME.2011.2162586

Lei Cao, Jie Li, Yaoru Sun, Huaping Zhu, & Chungang Yan. (2010). EEG-based vigilance analysis by using fisher score and PCA algorithm. *2010 IEEE International Conference on Progress in Informatics and Computing*, 175–179. https://doi.org/10.1109/PIC.2010.5687413

Lim, J.-H., Hwang, H.-J., Han, C.-H., Jung, K.-Y., & Im, C.-H. (2013). Classification of binary intentions for individuals with impaired oculomotor

function: `eyes-closed' SSVEP-based brain–computer interface (BCI). *Journal of Neural Engineering*, *10*(2), 026021. https://doi.org/10.1088/1741-2560/10/2/026021

Lotte, F., Congedo, M., Lécuyer, A., Lamarche, F., & Arnaldi, B. (2007). A review of classification algorithms for EEG-based brain-computer interfaces. *Journal of Neural Engineering*, *4*(2), R1–R13. https://doi.org/10.1088/1741-2560/4/2/R01

Lotze, M., & Halsband, U. (2006). Motor imagery. *Journal of Physiology-Paris*, *99*(4), 386–395. https://doi.org/10.1016/j.jphysparis.2006.03.012

Ludwig, K. A., Miriani, R. M., Langhals, N. B., Joseph, M. D., Anderson, D. J., & Kipke, D. R. (2009). Using a Common Average Reference to Improve Cortical Neuron Recordings From Microelectrode Arrays. *Journal of Neurophysiology*, *101*(3), 1679–1689. https://doi.org/10.1152/jn.90989.2008

Malechka, T., Tetzel, T., Krebs, U., Feuser, D., & Graeser, A. (2015). sBCI-Headset—Wearable and Modular Device for Hybrid Brain-Computer Interface. *Micromachines*, *6*, 291–311. https://doi.org/10.3390/mi6030291

Mathalon, D. H., Whitfield, S. L., & Ford, J. M. (2003). Anatomy of an error: ERP and fMRI. *Biological Psychology*, *64*(1–2), 119–141. https://doi.org/10.1016/S0301-0511(03)00105-4

Millan, Jd. R., Renkens, F., Mourino, J., & Gerstner, W. (2004). Noninvasive brain-actuated control of a mobile robot by human EEG. *IEEE Transactions on Biomedical Engineering*, *51*(6), 1026–1033. https://doi.org/10.1109/TBME.2004.827086

Mousavi, M., & de Sa, V. R. (2019). Spatio-temporal analysis of error-related brain activity in active and passive brain-computer interfaces. *Brain Computer Interfaces (Abingdon, England)*, *6*(4), 118–127. https://doi.org/10.1080/2326263x.2019.1671040

Nakasaki, H., Mitomi, T., Noto, T., Ogoshi, K., Hanaue, H., Tanaka, Y., Makuuchi, H., Clausen, H., & Hakomori, S. (1989). Mosaicism in the expression of tumor-associated carbohydrate antigens in human colonic and gastric cancers. *Cancer Research*, *49*(13), 3662–3669.

Nicolas-Alonso, L. F., & Gomez-Gil, J. (2012). Brain Computer Interfaces, a Review. *Sensors (Basel, Switzerland)*, *12*(2), 1211–1279. https://doi.org/10.3390/s120201211

Penaloza, C. I., Mae, Y., Kojima, M., & Arai, T. (2015). Brain signal-based safety measure activation for robotic systems. *Advanced Robotics*, *29*(19), 1234–1242. https://doi.org/10.1080/01691864.2015.1057615

Perrin, X., Chavarriaga, R., Colas, F., Siegwart, R., & Millán, J. del R. (Eds.). (2010). Brain-coupled Interaction for Semi-autonomous Navigation of an Assistive Robot. *Robotics and Autonomous Systems*. https://doi.org/10.1016/j.robot.2010.05.010

Pfurtscheller, G., Allison, B., Bauernfeind, G., Brunner, C., Solis Escalante, T., Scherer, R., Zander, T., Mueller-Putz, G., Neuper, C., & Birbaumer, N. (2010). The hybrid BCI. *Frontiers in Neuroscience*, *4*. https://www.frontiersin.org/articles/10.3389/fnpro.2010.00003

Pires, G., Castelo-Branco, M., Guger, C., & Cisotto, G. (2022). Editorial: Error-related potentials: Challenges and applications. *Frontiers in Human Neuroscience*, *16*. https://www.frontiersin.org/articles/10.3389/fnhum.2022.984254

Polich, J. (2007). Updating P300: An integrative theory of P3a and P3b. *Clinical Neurophysiology*, *118*(10), 2128–2148. https://doi.org/10.1016/j.clinph.2007.04.019

Quigley, M., Gerkey, B., Conley, K., Faust, J., Foote, T., Leibs, J., Berger, E., Wheeler, R., & Ng, A. (2010). *ROS: an open-source Robot Operating System*. 6.

Ramadan, R. A., & Vasilakos, A. V. (2017). Brain computer interface: Control signals review. *Neurocomputing*, *223*, 26–44. https://doi.org/10.1016/j.neucom.2016.10.024

Saab, J., Battes, B., & Grosse-Wentrup, M. (2011). *Simultaneous EEG Recordings with Dry and Wet Electrodes in Motor-Imagery*. 312–315.

Salazar-Gomez, A. F., DelPreto, J., Gil, S., Guenther, F. H., & Rus, D. (2017). Correcting robot mistakes in real time using EEG signals. *2017 IEEE International Conference on Robotics and Automation (ICRA)*, 6570–6577. https://doi.org/10.1109/ICRA.2017.7989777

Schalk, G., Wolpaw, J. R., McFarland, D. J., & Pfurtscheller, G. (2000). EEG-based communication: Presence of an error potential. *Clinical Neurophysiology: Official Journal of the International Federation of Clinical*

Neurophysiology, *111*(12), 2138–2144. https://doi.org/10.1016/s1388-2457(00)00457-0

Scherer, R., Schloegl, A., Lee, F., Bischof, H., Jansa, J., & Pfurtscheller, G. (2007). The self-paced graz brain-computer interface: Methods and applications. *Computational Intelligence and Neuroscience*, 79826. https://doi.org/10.1155/2007/79826

Schmidhuber, J. (2015). Deep Learning in Neural Networks: An Overview. *Neural Networks*, *61*, 85–117. https://doi.org/10.1016/j.neunet.2014.09.003

Schmidt, N. M., Blankertz, B., & Treder, M. S. (2012). Online detection of error-related potentials boosts the performance of mental typewriters. *BMC Neuroscience*, *13*(1), 19. https://doi.org/10.1186/1471-2202-13-19

Schwartz, A. B. (2004). Cortical Neural Prosthetics. *Annual Review of Neuroscience*, *27*(1), 487–507. https://doi.org/10.1146/annurev.neuro.27.070203.144233

Seeck, M., Koessler, L., Bast, T., Leijten, F., Michel, C., Baumgartner, C., He, B., & Beniczky, S. (2017). The standardized EEG electrode array of the IFCN. *Clinical Neurophysiology*, *128*(10), 2070–2077. https://doi.org/10.1016/j.clinph.2017.06.254

Sellers, E. W., Vaughan, T. M., & Wolpaw, J. R. (2010). A brain-computer interface for long-term independent home use. *Amyotrophic Lateral Sclerosis: Official Publication of the World Federation of Neurology Research Group on Motor Neuron Diseases*, *11*(5), 449–455. https://doi.org/10.3109/17482961003777470

Spüler, M., Bensch, M., Kleih, S., Rosenstiel, W., Bogdan, M., & Kübler, A. (2012). Online use of error-related potentials in healthy users and people with severe motor impairment increases performance of a P300-BCI. *Clinical Neurophysiology: Official Journal of the International Federation of Clinical Neurophysiology*, *123*(7), 1328–1337. https://doi.org/10.1016/j.clinph.2011.11.082

Suresh, S., Liu, Y., & Yeow, R. C.-H. (2015). Development of a Wearable Electroencephalographic Device for Anxiety Monitoring1. *Journal of Medical Devices*, *9*(3). https://doi.org/10.1115/1.4030553

Taeb, M., Shamsollahi, M. B., Ghassemi, F., & Asefisaray, B. (n.d.). *ERROR-RELATED POTENTIAL -IN BRAIN- ACTUATED WHEELCHAIR*. 1.

Tan, D., & Nijholt, A. (2010). Brain-Computer Interfaces and Human-Computer Interaction. In D. S. Tan & A. Nijholt (Eds.), *Brain-Computer Interfaces: Applying our Minds to Human-Computer Interaction* (pp. 3–19). Springer. https://doi.org/10.1007/978-1-84996-272-8_1

Venthur, B., Scholler, S., Williamson, J., Dähne, S., Treder, M. S., Kramarek, M. T., Müller, K.-R., & Blankertz, B. (2010). Pyff – A Pythonic Framework for Feedback Applications and Stimulus Presentation in Neuroscience. *Frontiers in Neuroscience*, *4*, 179. https://doi.org/10.3389/fnins.2010.00179

Wang, P., Lu, J., Zhang, B., & Tang, Z. (2015). A review on transfer learning for brain-computer interface classification. *2015 5th International Conference on Information Science and Technology (ICIST)*, 315–322. https://doi.org/10.1109/ICIST.2015.7288989

Wolpaw, J. R. (2002). Brain-computer interfaces (BCIs) for communication and control. *Proceedings of the 9th International ACM SIGACCESS Conference on Computers and Accessibility - Assets '07*, 1. https://doi.org/10.1145/1296843.1296845

Xavier Fidêncio, A., Klaes, C., & Iossifidis, I. (2022). Error-Related Potentials in Reinforcement Learning-Based Brain-Machine Interfaces. *Frontiers in Human Neuroscience*, *16*. https://www.frontiersin.org/articles/10.3389/fnhum.2022.806517

Yin, J., Jiang, D., & Hu, J. (2009). Design and application of brain-computer interface web browser based on VEP. *2009 International Conference on Future BioMedical Information Engineering (FBIE)*, 77–80. https://doi.org/10.1109/FBIE.2009.5405788

Zander, T., Lehne, M., Ihme, K., Jatzev, S., Correia, J., Kothe, C., Picht, B., & Nijboer, F. (2011). A Dry EEG-System for Scientific Research and Brain–Computer Interfaces. *Frontiers in Neuroscience*, *5*. https://www.frontiersin.org/articles/10.3389/fnins.2011.00053